# An electrochemical and computational study of tungsten(0) ferrocene complexes: observation of the mono-oxidized tungsten(0) ferrocenium species and intramolecular electronic interactions

Daniela I. Bezuidenhout[a*] Israel Fernández,[b*] Belinda van der Westhuizen,[a] Pieter J. Swarts,[c] and Jannie C. Swarts [c*]

[a] Department of Chemistry, University of Pretoria, Private Bag X20, Hatfield 0028, Pretoria, South Africa.

[b] Departamento de Química Orgánica I, Facultad de Química, Universidad Complutense, 28040-Madrid, Spain.

[c] Chemistry Department, University of the Free State, PO Box 339, Bloemfontein 9300, South Africa.
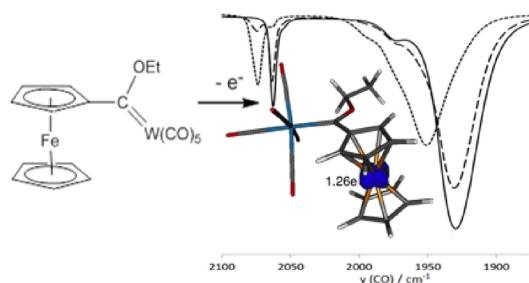
ABSTRACT

The series $[(CO)_5W=C(XR)Fc]$, **1** (XR = OEt) and **3** (XR = NHBu) as well as $[(CO)_5W=C(XR)-Fc'-(XR)C=W(CO)_5]$, **2** (XR = OEt) and **4** (XR = NHBu) of mono- and biscarbene tungsten(0) complexes with Fc = $Fe^{II}(C_5H_5)(C_5H_4)$ for monosubstituted derivatives and Fc′ = $Fe^{II}(C_5H_4)_2$ for disubstituted derivatives were synthesized and characterized spectroscopically. The oxidized ferrocenium complex $[\mathbf{1}^+]\cdot PF_6$ was also synthesized and characterized. Electrochemical and computational studies were mutually consistent in confirming the sequence of redox events for the carbene derivatives **1 − 4** as first a carbene double bond

reduction to a radical anion, $^-$W-C•, at peak cathodic potentials smaller than -2 V, then a ferrocenyl group oxidation in the range $0.206 < E^{o'} < 0.540$ V and finally an electrochemically irreversible three-electron W(0) oxidation at $E_{pa} > 0.540$ V vs. FcH/FcH$^+$ in CH$_2$Cl$_2$ / [(^{n}Bu$_4$)N][PF$_6$]. This contrasts the sequence of oxidation events in ferrocenylcarbene complexes of chromium where Cr(0) is first oxidised in a one electron transfer process, then the ferrocenyl group, and finally formation of a Cr(II) species. The unpaired electron of the reductively formed radical anion is mainly located on the carbene carbon atom. Electronic interactions between two carbene double bonds (for biscarbenes **2** and **4**) as well as between two W centers (for **4**) were evident. Differences in redox potentials between the "a" and "b" components of the three-electron W oxidation of **4** in CH$_2$Cl$_2$ or CH$_3$CN / [(^{n}Bu$_4$)N][PF$_6$] are $\Delta E^{o'} = E_{pa\ W(0)\ oxd\ 1b} - E_{pa\ W(0)\ oxd\ 1a}$ = ca. 51 and 337 mV respectively. Tungsten oxidation was restricted to a W$^{0/II}$ couple in CH$_2$Cl$_2$ / [(^{n}Bu$_4$)N][B(C$_6$F$_5$)$_4$]. From the computational results, the short-lived W(II) species were observed to be stabilized by agostic CH···W interactions.

Introduction

Based on its reversible electrochemical signature, ferrocene derivatives are researched as molecular sensors,[1] in energy transfer processes,[2] as catalysts[3] and even in anticancer research.[4] Fischer carbene complexes are versatile organometallics with valuable applications in organic and organometallic synthesis as well as in the fields of bioorganometallics and materials chemistry.[5] Recently, computational studies especially enhanced the understanding of this group of organometallic compounds substantially.[6]

The first examples of ferrocenyl carbene complexes of the group 6 transition metals, $[(CO)_5Cr=C(OR)Fc]$ (R = Me, Et), were synthesized to study the electronic effects of the ferrocenyl substituent on the carbene ligand as part of an investigation into the electron withdrawing nature of metal carbonyl carbene groups.[7] Early hints of the increased stability and chemodirecting steric effect of ferrocenyl carbene complexes were reported by Dötz et al.[8] Reaction of these ferrocenyl carbene complexes with tolane gave unexpected furanoid products over the customary Dötz benzannulation that yields chromium-coordinated hydroquinones.[9]

Our recent investigation into the electrochemical behavior of Fischer carbene complexes of the type $[(CO)_5Cr=C(XR)Ar]$ (XR = OEt, NHBu or NHPr; Ar = 2-thienyl (Th), 2-furyl (Fu) or ferrocenyl (Fc)), revealed the formation of dicationic Cr(II) species formed upon two consecutive one-electron oxidation processes.[10] These dicationic carbene complexes are characterized by an unusual bonding situation as they are stabilized by CH···Cr agostic interactions.[11] Strikingly, for the biscarbene complexes $[(CO)_5Cr=C(OEt)-Fc'-(OEt)C=Cr(CO)_5]$ (Fc' = ferrocen-1,1'-diyl), two resolved $Cr^{0/I}$ couples were observed. It was observed that intramolecular electronic interactions between the two Cr(0) centers is much more effective in biscarbene complexes linked together by a ferrocen-1,1′-diyl functionality,[12] since the biscarbene complexes with 2,5-thiendiyl or 2,5-furadiyl spacers did not display the split of the $Cr^{0/I}$ couple into two components. Rather, the redox processes in these heteroaryl biscarbene complexes are two-electron transfer processes that comprise two simultaneously occurring but independent one-electron transfer steps, one for each Cr(0) center.

In contrast to our findings that the $Cr^{I/0}$ and $Cr^{II/I}$ redox couples in Fischer carbene complexes are at potentials that may differ as much as 0.75 V,[10,11] tungsten(0) carbene complexes were reported to be oxidized to tungsten(II) carbene complexes either by a single two-electron transfer process

3

or by two unresolved (overlapping) one electron transfer processes.[13] Previous electrochemical studies[14] on the redox behavior for chromium(0) and tungsten(0) carbene complexes did not identify a $M^{II/I}$ couple, nor did they comment on the now firmly established reduction of the chromium carbene double bond, Cr=C to the radical anion $^-$Cr-C•.[10,11] It is clear that the electrochemical behavior of chromium(0) and tungsten(0) Fischer carbene complexes and the driving forces behind it may not be so similar as was accepted till now. To probe the differences between chromium and tungsten carbenes, including the possibility of metal-metal communication between the tungsten pentacarbonyl termini, we synthesized the ethoxycarbene complexes $[(CO)_5W=C(OEt)Fc]$ (**1**),[15] $[(CO)_5W=C(OEt)Fc'(OEt)C=W(CO)_5]$ (**2**), and the new aminocarbene analogues, $[(CO)_5W=C(NHBu)Fc]$ (**3**), and $[(CO)_5W=C(NHPr)Fc'(NHPr)C=(CO)_5]$ (**4**) (Scheme 1). In addition, the isolation of the monocationic salt, $[\mathbf{1^+}]\cdot\mathbf{PF_6}$, was achieved. An electrochemical analysis, supported by density functional theory (DFT) calculations and spectroscopic analyses, are reported and results are compared to highlight the differences between Cr and W analogues.
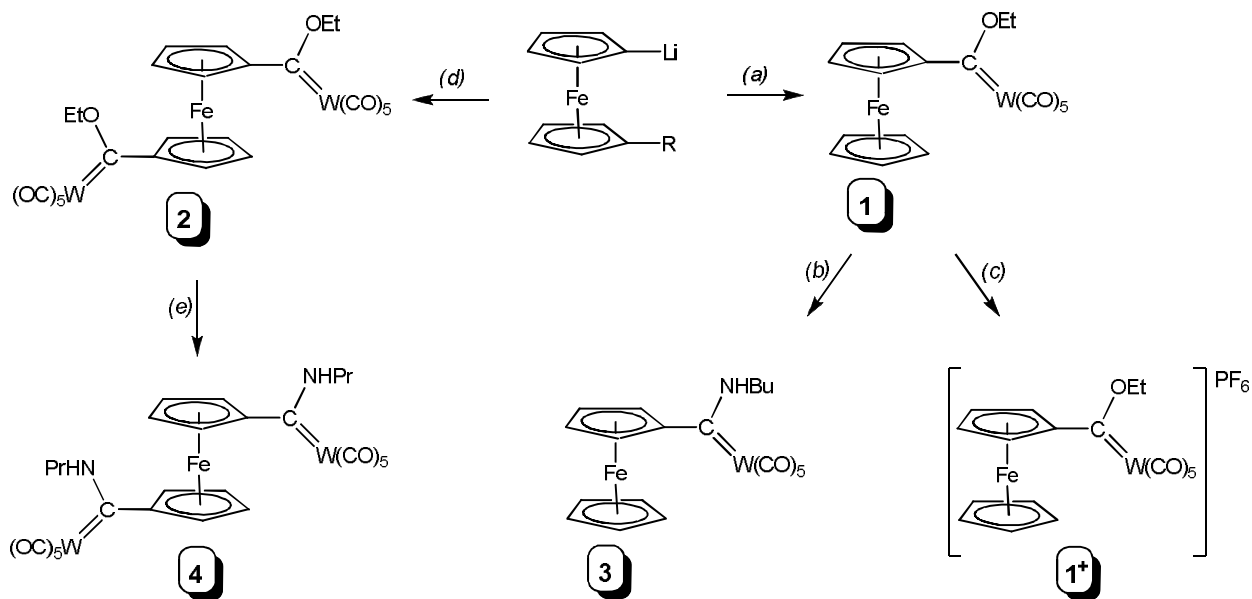
Scheme 1. Synthesis of ferrocenyl mono- and biscarbene tungsten complexes; Reagents and conditions: (a) (i) 1 eq FcLi (R = H), 1eq [W(CO)$_6$], thf, -50°C; (ii) 1.3eq Et$_3$OBF$_4$, CH$_2$Cl$_2$, -30°C; (b) 1.1eq NH$_2$Bu, Et$_2$O, rt; (c) 1eq AgPF$_6$, CH$_2$Cl$_2$, -35°C; (d) (i) 1eq Fc'Li$_2$ (R = Li), 2eq [W(CO)$_6$], thf, -50°C; (ii) 2.5eq Et$_3$OBF$_4$, CH$_2$Cl$_2$, -30°C; (e) 2.2eq NH$_2$Pr, Et$_2$O, rt.

Results and Discussion

Synthesis and spectroscopic characterization of complexes 1 - 4.

Ferrocenyllithium[16] was reacted with [W(CO)$_6$] in the classic Fischer route to carbene complexes (Scheme 1), followed by alkylation with Et$_3$OBF$_4$[17] to yield the known complex **1** [(CO)$_5$W=C(OEt)Fc].[15] Following the procedure described for the synthesis of the chromium analogues, reaction of two equivalents of tungsten carbonyl and 1,1'-dilithioferrocene[18] yielded the tungsten bisacylate. Quenching of the reaction was achieved with excess of oxonium salt, to yield the novel bridging ferrocen-1,1'-diyl biscarbene complex, **2**

[(CO)$_5$W=C(OEt)Fc′(OEt)C=W(CO)$_5$]. Both the monocarbene complex **1** and biscarbene complex **2** were aminolysed[19] with *n*-butylamine or *n*-propylamine, respectively, to yield the new complexes [(CO)$_5$W=C(NHBu)Fc] (**3**) and [(CO)$_5$W=C(NHPr)Fc′(NHPr)C=W(CO)$_5$] (**4**). These tungsten carbene complexes displayed NMR and FTIR spectroscopic properties similar to that observed for their chromium analogues.[10,11] Upfield shifts of the ferrocenyl-H$_\alpha$ in the case of the aminocarbene complexes **3** and **4** (4.24 and 4.56 ppm, respectively) compared to the ethoxycarbenes **1** and **2** (4.98 and 5.02 ppm, respectively), upfield ^{13}C NMR shifts of the carbene carbon resonances of the aminocarbenes compared to the ethoxycarbenes (eg. **3**, 249.1 ppm compared to **1**, 304.3 ppm) and decreased carbonyl stretching frequencies of the overlapping A′$_1$ and E-modes for the aminocarbenes compared to the ethoxy analogues (**3**, 1922 cm^{-1}; **4**, 1920 cm^{-1} vs. **1**, 1932 cm^{-1}; **2**, 1935 cm^{-1}) are all indicators of the increased donating ability of the amino-substituents towards stabilizing the electrophilic carbene carbon atom.[19] This is due to the contribution of imine formation to the C$_{carbene}$-N bond (Figure 1), which results in the formation of both *syn*- and *anti*-configurational isomers around the abovementioned C$_{carbene}$-N bond.[10,11] However, as for the Cr-derivatives, the steric bulk of the ferrocenyl carbene substituent precludes the formation of both isomers, and only the *syn*-isomer can be observed by NMR. [20]
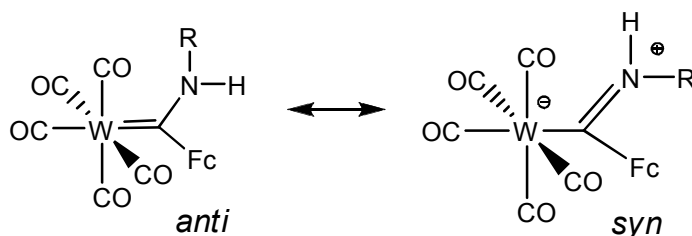

Figure 1. Stabilization of Fischer aminocarbene complexes via imine formation. For both **3** and **4**, only the *syn* rotamer is observed.

During the electrochemical investigation, we observed more positive oxidation potentials for the tungsten carbene complexes compared to the chromium analogues, in accordance with the higher hyperpolarizability of the tungsten complexes.[13] For our bimetallic complexes, however, this meant that in contrast to the chromium ferrocenyl complexes,[10] the first oxidation process corresponds to the $Fe^{II/III}$ couple and not to the tungsten carbonyl moiety (see Electrochemistry Section). This encouraged us to perform the chemical oxidation of **1** with $AgPF_6$ (see Scheme 1) to gain insight into the properties of the ferrocenium cation **1**$^+$. For the Cr-analogues, although this first $Cr^{0/I}$ oxidation proved reversible, the formed chromium +1 cation could not be isolated. After the addition of 1 equivalent of $AgPF_6$ to a solution of **1** in CH_2Cl_2 at -35 °C, an immediate color change from red to brown was observed. While the solution was allowed to warm to room temperature, IR and NMR data had to be collected for **[1**$^+$**]•PF**$_6$ within 10 minutes before decomposition of **1**$^+$ occurred. Spectroscopically it could be seen (Figure 2) that much of **1**$^+$ reverted back to **1**, probably by the capture of an electron from any electron-rich species in solution such as the free electron pairs on CO or OEt. To the best of our knowledge, no other isolated example of such a chemically oxidized ferrocenium Fischer carbene complex has been reported.

The IR spectra (Figure 2) clearly illustrate the shift of the carbonyl stretching frequencies from 1932, 1976 and 2063 cm^{-1} for **1** to 1953, 1998 and 2074 cm^{-1} for **1**$^+$. The magnitude of the wavenumber shifts (21, 22 and 11 cm^{-1} for the E overlapping with A'_1, B and A''_1 bands respectively), is smaller than the shift of more than 100 cm^{-1} that is expected for oxidation of metal-carbonyl-based W(0) to W(I). Instead, it corresponds to an inductive effect accompanying the oxidation of the ferrocenyl Fe(II) substituent to a ferrocenium Fe(III) species. During this oxidation, the highly electron donating ferrocenyl group having a group electronegativity of χ_{Fc}

= 1.87 converted to an electron-withdrawing ferrocenium species (χ_{Fc+} = 2.82) almost as strong

as the CF$_3$ group (χ_{CF3} = 3.01).[21] This observation is corroborated by the electrochemical data

presented below. In addition, previous calculations reported the stabilization of the partially

empty carbene carbon p_z atomic orbital by donation from a doubly-occupied d-orbital of iron.[22]

Thus, with the removal of an electron from this atomic orbital, the donation is lowered, reducing

the electron density of the W=C bond. Consequently, the π-backdonation to the π* orbital of the

CO is also reduced with resulting higher C=O bond strength and higher CO stretching

frequencies. The ^{1}H NMR spectrum recorded did not show any ferrocenyl resonances, even

when recorded in a spectral window of up to 50 ppm, although the ferrocenium chemical shift is

reported at δ31 ppm.[23] Presumably this can be ascribed to the paramagnetic nature of cation **1**$^+$.

The presence of the PF$_6$ counter anion is confirmed by the upfield shifts of the resonances in the

^{31}P and ^{19}F NMR spectra in CD$_2$Cl$_2$, where for **[1$^+$]•PF$_6$** δ ^{31}P = -149.6 and δ ^{19}F = -85.4 ppm.

The characteristic pentacarbonyl metal υ(CO)-pattern[24] indicates that no CO-ligand had been

substituted by a coordinating PF$_6$-moiety.
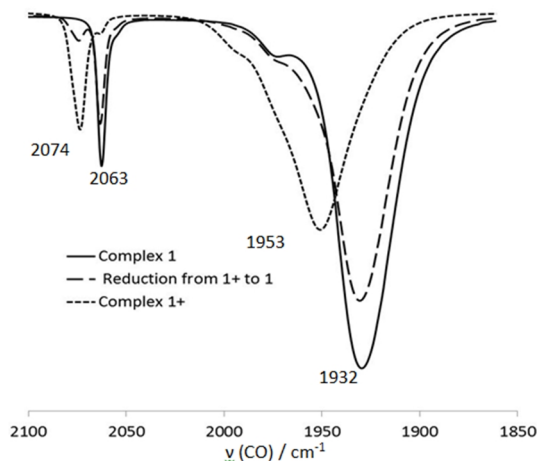
**Figure 2.** IR spectra demonstrating the carbonyl vibrations observed for complexes **1**, **[1$^+$]•PF$_6$** and the regeneration

of **1**.

Electrochemistry and computational analyses

Cyclic voltammetry (CV), linear sweep voltammetry (LSV), and Osteryoung Square Wave voltammetry (SW) were first conducted on 0.5 mmol·dm^{-3} solutions of **1 – 4** in dry, oxygen-free CH$_2$Cl$_2$ utilizing 0.1 mol·dm^{-3} [N(^{n}Bu)$_4$][PF$_6$] as supporting electrolyte. Data are summarized in Table 1, CV's are shown in Figures 4, 5 and 6.

At far negative potentials, the carbene double bond of the mono-ethoxycarbene derivative **1** was reduced electrochemically reversibly (ΔE = 63 mV), but chemically irreversibly (i_{pa}/i_{pc} = 0.56) in a one-electron transfer redox process to a radical anion at $E^{o'}$ = ½(E$_{pa}$ + E$_{pc}$) = -2.076 V vs. FcH/FcH$^+$ (Table 1, Figure 4). Electrochemical and chemical reversibility is theoretically characterized by peak potential differences of ΔE = E$_{pa}$ – E$_{pc}$ = 59 mV and current ratios i$_{pa}$/i$_{pc}$ approaching unity.[25] As is usual for Fischer carbene complexes,[6] the LUMO of complex **1** is mainly located at the p_z atomic orbital of the carbene carbon atom (Figure 3). Therefore, it should be expected that the one-electron reduction process should lead to the radical anion **1·$^-$** whose unpaired electron remains mainly located on that carbon atom. Indeed, the computed spin density on **1·$^-$** indicates a value of 0.57 e on the carbene carbon atom thus suggesting a $^-$W-C· species as reduction product. The remaining electron density is mainly localized at the iron center (0.27e) which further confirms the orbital interaction between the ferrocenyl group and the carbene carbon atom.[22] Similar electron density was computed for the analogous (CO)$_5$Cr=C(OEt)Fc carbene complex at the same level of theory (0.57e at the carbene carbon atom), thus indicating that the one-electron reduction process is similar in both types of complexes.

HOMO (1)   **LUMO (1)**   **1·⁻**
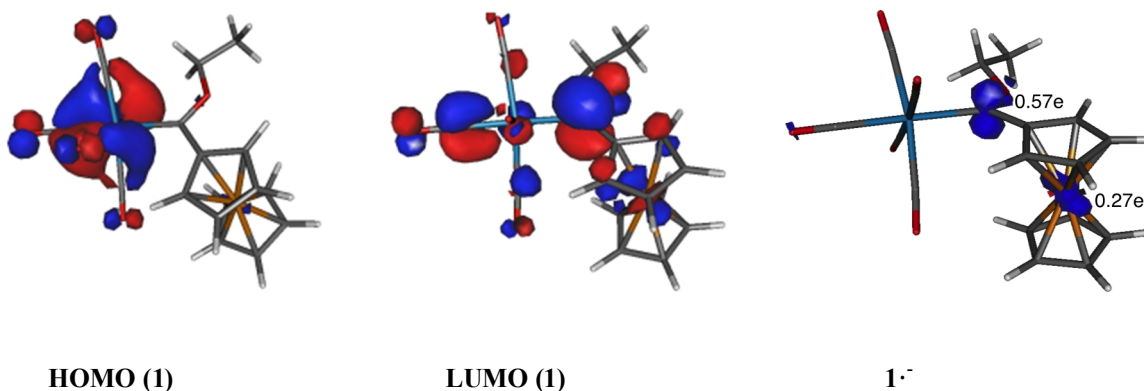
Figure 3. Frontier Molecular Orbitals of **1** and computed spin density on **1**$^{\cdot-}$.

The bisethoxy complex **2** exhibited two W=C reductions at waves I_a and I_b in the CV's shown in Figure 4 to $^-$W-C· with formal reductions potentials being separated by $\Delta E^{o'} = E^{o'}_{wave\ Ib} - E^{o'}_{wave\ Ia}$ = 433 mV. This relatively large separation in reduction potentials illustrates noticeable interactions between the two carbene moieties and leads to the general reductive scheme shown in equation 1. The first carbene reduction associated with wave I_a is electrochemically reversible but the second is not (Figure 4 and Table 1).

$$\textbf{2}^{2\bullet,2-} \underset{+e^-}{\overset{\textbf{wave I}_b}{\longleftarrow}} \textbf{2}^{\bullet,-} \underset{+e^-}{\overset{\textbf{wave I}_a \quad -e^-}{\rightleftharpoons}} \textbf{2} \quad (1)$$
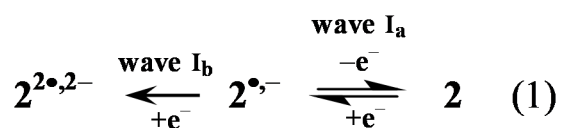
The radical anion notation in equation 1 is explained by noting that $\textbf{2}^{\bullet\,-} = [(CO)_5(^-W\text{-}C^{\bullet})(OEt)\text{-}Fc'\text{-}(OEt)C=W(CO)_5]$. Different reduction potentials for symmetrical complexes in which mixed-valent intermediates are generated (for **2,** this refers to $\textbf{2}^{\bullet\,-}$) are well known in systems that allow some form of electronic interaction between the redox centers; these may include electrostatic or through-bond conjugated paths.[26]

In contrast to the OEt derivatives **1** and **2**, the new NHBu monocarbene **3** showed no carbene reduction within the potential window of the solvent in the presence of $[N(^nBu)_4][PF_6]$. This agrees with the computed energy of the corresponding LUMO (-2.64 and -2.25 eV for **1** and **3**, respectively) which suggests that the less negative energy of the LUMO of **3** is translated into a more negative reduction potential. The biscarbene-NHPr derivative **4**, showed a single carbene reduction at -2.293 V in the CV at wave I (Figure 4), but the current was more than four times (3.71/0.90) larger than that expected for a one-electron transfer processes. A one-electron transfer process in this system requires ½[i(wave Fc+1a)/4+i(wave 1b)/3] = 0.90 µA. The large observed current (3.71 µA) is thought to be due to significant amounts of substrate being deposited on the surface of the electrode during reduction but because this wave is close to the potential at which cathodic discharge caused by solvent reduction takes place, the large increase in current may also originate from an E_rC_{cat} process by which **4** catalyses the reduction of CH_2Cl_2. A repeat experiment utilizing **4** as analyte in CH_3CN as solvent (Figure S3, Supplementary Material, Table 1) confirmed the second carbene moiety is reduced at a potential ca. 0.27 V lower than the first. This observation also suggests some form of electronic interaction between two carbene moieties observed for **2** but completely contrasts the observations described for the chromium complex $[(CO)_5Cr=C(OEt)-Fc'-(OEt)C=Cr(CO)_5]$.[10,11] For this analogous Cr carbene complex, under the same experimental conditions, no splitting of Cr=C carbene reduction into two components "a" and "b" could be detected. Very few studies describe the electrochemical reduction of the W=C double bond,[14] although the *in situ* generation of the radical anion by chemical single electron transfer agents have been reported.[27] Consistent with NHR (R = Bu, Pr) being a more powerful electron-donating group than OEt, the NHPr group

shifted the wave I_a peak cathodic potential, E_{pc}, of the bis W=C species **4** compared to **2** with

$$\Delta E_{pc} = E_{pc, OEt, \textbf{2}} - E_{pc, NHBu, \textbf{4}} = -1.773 - (-2.293) = 0.520 \text{ to more negative potentials.}$$

Table 1. Cyclic voltammetry data of 0.5 mmol·dm^{-3} solutions of the monocarbene [(OC)$_5$W=C(Fc)(X)] complexes **1** and **3** and biscarbene [(OC)$_5$W=C(X)-Fc'-(X)C=W(CO)$_5$] complexes **2** and **4** in CH$_2$Cl$_2$ containing 0.1 mol·dm^{-3} [N(^{n}Bu)$_4$][PF$_6$] or 0.2 mol·dm^{-3} [N(^{n}Bu)$_4$][B(C$_6$F$_5$)$_4$] as supporting electrolyte at a scan rate of 100 mV s^{-1} and 20 ^{o}C. Potentials are relative to the FcH/FcH$^+$ couple.

Complex	Peak no.	i_{pa}/μA, i_{pc}/i_{pa} [N(^{n}Bu)$_4$][PF$_6$]	$E^{o'}$/V, ΔE/mV [N(^{n}Bu)$_4$][PF$_6$]	$E^{o'}$/V, ΔE/mV [N(^{n}Bu)$_4$][B(C$_6$F$_5$)$_4$]	i_{pa}/μA, i_{pc}/i_{pa} [N(^{n}Bu)$_4$][B(C$_6$F$_5$)$_4$]
1, Fc X = OEt	I(=)	3.23,^{b} 0.56	-2.076, 63	-2.119, 100	7.02,^{b} 0.71
	(Fc)	3.38, 0.85	0.285, 90	0.307, 82	5.61 0.93
	1(W$^{0/III}$)	10.01, -	0.809,^{d} -	(W$^{0/II}$)1.105,^{d,i} -	11.58, -
2, Fc' X = OEt	D^f	0.76,^{b} -	-2.409,^{c} -		
	Ib(=)	1.64,^{b} -	-2.206,^{c} -	-2.222,^{c} -	2.80,^{b} -
	Ia(=)	1.73,^{b} 0.40	-1.773, 67	-1.811, 74	3.02,^{b} 0.51
	(Fc)	1.62, 0.84	0.510, 86	0.513, 82	2.82, 0.64
	1(2xW$^{0/III}$)	9.56, 0.15	0.766, 142	(2xW$^{0/II}$) 0.922,^{i} -	(2xW$^{0/II}$) 9.99, -
3, Fc X =NHBu	I(=)	-^{a}, -^{a}	-^{a}, -^{a}	-2.580,^{c} -	9.71,^{b} -
	(Fc)	2.67, 0.88	0.206, 92	0.289, 80	4.23, 0.67
	1(W$^{0/III}$)	7.94, 0.11	0.611, 293	(W$^{0/II}$) 0.950,^{d,i} -	(W$^{0/II}$) 8.10,^{d} -
4, Fc' X = NHPr	I(=)	3.71,^{b} -	-2.293,^{c} -	-2.285,^{c} -	6.84 ^{b}, -
	(Fc)+1$_a$(W$^{0/1III}$)	3.53, -	0.540,^{e,h} -	(Fc)+1$_a$(W$^{0/1III}$) 0.580,^{d,e,h}	7.20, -
	1$_b$(W$^{0/III}$)	2.76, -	0.591,^{d} -	-	(2xW$^{0/II}$) 5.45, -
	D^f	0.55, -	1.000,^{d} -	(1$_b$ W$^{0/II}$) 0.792,^{d,i} -	-
4,^{g} Fc' X = NHPr CH$_3$CN^g	I$_b$(=)	1.30 ^{b}, -	-2.458,^{c} -		
	I$_a$(=)	3.38 ^{b}, -	-2.185,^{c} -		
	(Fc)+1$_a$(W$^{0/1III}$)^i	3.40, 0.31	0.408, 80		
	1$_b$(W$^{0/III}$)^i	4.69, 0.21	0.745, 100		

(a) No peak detected within the solvent potential window; (b) i_{pc} and i_{pa}/i_{pc} values to maintain the current ratio convention of i(forward scan)/i(reverse scan); (c) E_{pc} value, no E_{pa} detected. (d) E_{pa} value, no E_{pc} detected; (e) Estimations only; (f) Peaks labeled "D" represent decomposition processes of either the $^-$W-C· radical anions that was generated at the redox processes labeled "I" or of W(III) generated at wave "1b"; (g) The supporting electrolyte changed to BARF = [NBu$_4$][B(C$_6$F$_5$)$_4$] (0.2 mol·dm^{-3}) or the solvent changed to CH$_3$CN; (h) a very weak Fc reduction peak was observed at E_{pc} = 0.357, i_{pa} = 0.3 μA. In the presence of [NBu$_4$][B(C$_6$F$_5$)$_4$] a much stronger Fc reduction wave was observed at E_{pa} = 0.497, i_{pa} = 3.75 μA. (i) In the presence of [NBu$_4$][B(C$_6$F$_5$)$_4$] (0.2 mol·dm^{-3}) W oxidation is a two-electron transfer process, while in the presence of CH$_3$CN, or [N(^{n}Bu)$_4$][PF$_6$] it is a three-electron transfer process.

The next redox process observed for **1 – 4** is the chemically and electrochemically one-electron reversible oxidation of ferrocene which is associated with wave Fc in Figure's 4, 5 and 6, and Table 1. The Fc wave in these CV's is followed by the W oxidation processes (wave 1) which in CH_2Cl_2 / $[(^nBu_4)N][PF_6]$ involves a three-electron transfer process (Figure 4). This oxidation of the ferrocenyl group in tungsten carbenes at lower potentials than that of W oxidation contrasts with the behavior of the analogues chromium carbenes $[(OC)_5Cr=C(Fc)(OEt)]$ and $[(OC)_5Cr=C(OEt)-Fc'-(OEt)C=Cr(CO)_5]$ where the ferrocenyl group was oxidized *after* oxidation of the Cr(0) center to Cr(I).[10,11] The second oxidation of Cr(I) to Cr(II) follows after the ferrocenyl oxidation, and also contrasts with the three-electron closely-overlapping W oxidation under the same experimental conditions. The resolution between Fc and tungsten (wave 1) oxidation processes, expressed as $\Delta E_{pa} = E_{pa, W} - E_{pa, Fc}$, is better in mono- than in biscarbene tungsten complexes, and also in OEt than in NHR complexes. For **4**, the Fc wave was superimposed onto a W-oxidation wave (Figure 4).

An important consequence of the ferrocenyl moiety being oxidized before the W center is that when the W center is oxidized, it is under the influence of the ferrocenium species, Fc^+, which is almost as electron-withdrawing as a CF_3 group ($\chi_{Fc} = 2.82$; $\chi_{CF3} = 3.01$).[21] This shifts the W redox process to more positive potentials than would be expected for other compounds where the linking group is not so strongly electron-withdrawing, e.g. for $-CH_2-$. The one-electron ferrocenyl oxidation process was useful to identify the number of electrons that is transferred during tungsten oxidation.

Tungsten oxidation is associated with wave 1 in Figures 4, 5, 6 and Table 1. Since the peak anodic current ratio between wave Fc and wave 1 in the CV of **1** was $10.01/3.38 = 2.96 = 3$, indications are that W(0) is oxidized irreversibly (no i_{pc} detected) in three consecutive and

overlapping one-electron transfer steps, apparently to a W(III) species (Figure 4, Table 1). This contrasts a study by Maiorana and co-workers who reported a few years ago that W in $[(OC)_5W=C(CH_3)(X)]$ with X = substituted morpholino and other amine derivatives undergo a two-electron oxidation in CH_2Cl_2 in the presence of 0.1 mol·dm^{-3} $[(^nBu_4)N][ClO_4]$ as supporting electrolyte.[13] Figure 5 highlights the CV's of **1** at different scan rates, and more importantly, the LSV at 1mV·s^{-1}. The LSV was mutually consistent with CV i_{pa} current ratios between wave Fc and wave 1 at scan rates of 100, 200, 300, 400 and 500 mV·s^{-1} in indicating that the total W oxidation involves the flow of three electrons. With our observation of a three-electron transfer W oxidation, it follows that in the biscarbene **2**, possessing two tungsten centers, a total of six electrons being transferred during tungsten oxidation should be observed. This was confirmed by the measured i_{pa} values (Figure 4, $i_{pa,wave\ 1}/i_{pa,wave\ Fc}$ = 9.56/1.62 = 5.90 ≈ 6, Table 1). Although the CV of **2** showed electronic interactions between the two carbene double bond centers by means of the splitting of wave I into two components "a" and "b", no resolution between the irreversible oxidations of the two W centers of **2** could be detected (Figure 4). However, a very weak reduction of oxidized W was detected at wave 1_r during the cathodic sweep, Figure 4, Table 1. The current was, however, small with i_{pc}/i_{pa} = 0.15; ΔE = 143 mV.

An LSV of **2** (Supplementary Information, Figure S1) showed that the oxidation of the second tungsten center results in a species that is unstable on LSV time scale. Only the first 3-electron oxidation could be detected before compound decomposition took place. The peak anodic current of wave 1 in the CV of the mono NHBu tungsten carbene **3** also estimates a three electron transfer step during W oxidations but the LSV shown in Figure 4 highlights new information. On LSV timescale, the first two electrons during W oxidation are transferred fast in two unresolved one-electron redox processes, but the different slope observed for the third

electron that was transferred shows this redox step to be slower than the first two electron transfer steps. The LSV splitting of wave 1 (W-oxidation) into two components "a" (a two electron process) and "b" (a one-electron process) for **3** allows for a meaningful comparison with chromium carbene analogues $[(OC)_5Cr=C(XR)(Ar)]$ and $[(OC)_5Cr=C(XR)-Ar'-(XR)C=Cr(CO)_5]$ with XR = OEt , NHBu or NHPr and Ar or Ar' = thienyl, furyl or ferrocenyl.[10,11] In these Cr carbene derivatives, Cr(0) is oxidized in two separate one-electron transfer steps and exhibits $\Delta E_{pa} = E_{pa,Cr(I/II)} - E_{pa,Cr(0/I)}$ peak potential separations larger than 0.5 V.[10,11] For the present W-series, indications are that W(0) is first oxidized in a two electron step followed by a second one-electron oxidation. In all compounds studied, these steps overlap on CV timescale, but on LSV timescale, for **3**, $\Delta E_{pa} = E_{pa,W(II/III)} - E_{pa,W(0/II)}$ peak separations are estimated from Figure 4 to be approximately 90 mV.
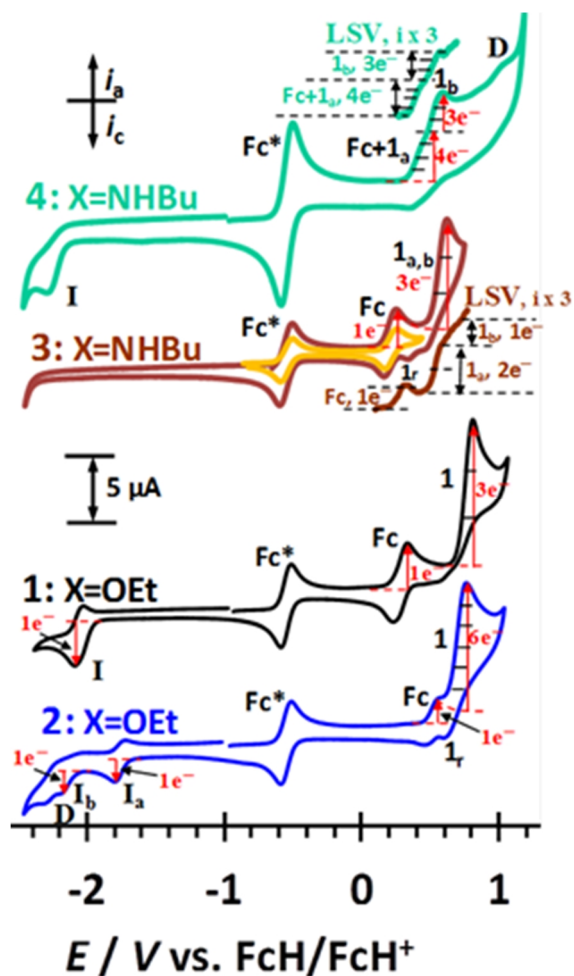
Figure 4. CV's of 0.5 mmol.dm^{-3} solutions of the monocarbene $[(OC)_5W=C(Fc)(XR)]$ complexes **1** (black) and **3** (brown) and biscarbene complexes $[(OC)_5W=C(XR)-Fc'-(XR)C=W(CO)_5]$ **2** (blue) and **4** (green) in CH_2Cl_2 containing 0.1 mol.dm^{-3} $[N(^nBu)_4][PF_6]$ as supporting electrolyte at a scan rate of 100 mV s^{-1} and 20 ^oC. LSV's are also shown for **3** and **4**. Fc* = decamethylferrocene = internal standard. Under these conditions, each W center is ultimately involved in a three-electron transfer redox process.

A small cathodic peak associated with wave 1 was also observed for **3** at wave 1_r but again irreversible W oxidation was implied by virtue of $i_{pc}/i_{pa} = 0.11$ and $\Delta E = 293$ mV. The CV's of the NHBu biscarbene **4** showed oxidation of the ferrocenyl group and one of the two W centers occurred simultaneously. For **4**, the oxidation of the second W center was resolved from the first

16

by ca. $\Delta E_{pa} = E_{pa, \text{ wave (1b+Fc)}} - E_{pa, \text{ wave 1a}} = 51$ mV. The ratio $i_{pa, \text{ wave (1b+Fc)}} : i_{pa, \text{ wave 1a}}$ in the CV as well as the LSV (Figure 4) was found to be 4:3 which again showed W oxidation involves three electrons.
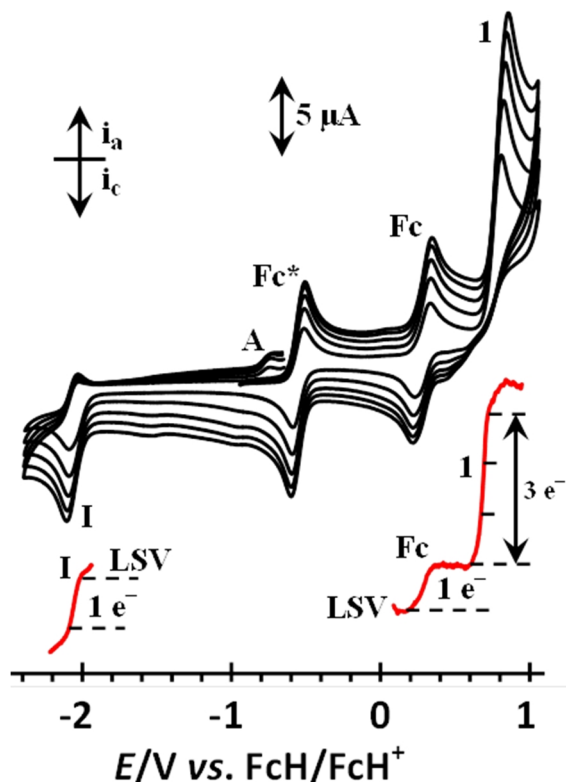
Figure 5. CV's of 0.5 mmol·dm^{-3} solutions of the [(OC)$_5$W=C(Fc)(OEt)], **1**, in CH$_2$Cl$_2$ containing 0.1 mol·dm^{-3} [N(^{n}Bu)$_4$][PF$_6$] as supporting electrolyte at a scan rate of 100 (smallest currents), 200, 300, 400 and 500 mV·s^{-1} and 20 ^{o}C. The LSV's show that the W center is involved in a three-electron transfer redox process, while both the ferrocenyl group and the carbene double bond involves one-electron flow. Fc* = decamethylferrocene. A = decomposition product peak.

To understand why our results indicating an irreversible three-electron W(0) oxidation differed from those of Maiorana, who observed a two-electron W oxidation,[13] complexes **1 – 4** were also studied under different conditions utilizing first 0.1 mol·dm^{-3} [(^{n}Bu$_4$)N][B(C$_6$F$_5$)$_4$] as supporting electrolyte, see Table 1 for electrochemical data. The Geiger electrolyte, [(^{n}Bu$_4$)N][B(C$_6$F$_5$)$_4$], is

known to minimize ion pair formations of the type $(cation)^{+} \cdots ^{-}[B(C_6F_5)_4]$ where $(cation)^{+}$ represents any electrochemically generated cation. Such ion pair formations frequently cause oxidation potentials of cationic species to move to different values.[28] In addition, use of this electrolyte allows the observation of unstable intermediate redox states of, for example, the ruthenocenium species $[Ru^{III}(C_5H_5)_2]^{+}$.[29] Use of other solvents or electrolytes invariably causes over oxidation of ruthenocene to a Ru(IV) species.[30]

Figure 6 shows a CV and LSV's of **2** utilizing $0.1 \ mol \cdot dm^{-3}$ $[(^nBu_4)N][B(C_6F_5)_4]$ as supporting electrolyte. The first obvious difference is that in CH_2Cl_2, but in the presence of $[(^nBu_4)N][B(C_6F_5)_4]$ as supporting electrolyte, resolution between the ferrocenyl oxidation and the two overlapping W(0) oxidations are markedly increased. The differences in the oxidation potentials of these two processes are $\Delta E^{o'} = E_{pa,W(0) \ oxd, \ 1} - E_{pa,Fc \ oxd} = 284 \ mV$ in CH_2Cl_2 containing $[(^nBu_4)N][PF_6]$ and $368 \ mV$ in CH_2Cl_2 containing $[(^nBu_4)N][B(C_6F_5)_4]$. More importantly, the LSV as well as i_{pa} current ratios for waves Fc and 1 in the presence of $[(^nBu_4)N][B(C_6F_5)_4]$, shows a two-electron tungsten oxidation, the same as reported by Maiorana.[13] All the other complexes in the present compound series **1 – 4** also showed the two-electron $W^{0/II}$ couple when the supporting electrolyte was $[(^nBu_4)N][B(C_6F_5)_4]$, see Table 1 and Supplementary Information, Figures S3 and S4.

An additional experiment utilizing CH_3CN as solvent was also performed on **4** because the coordination power of acetonitrile (Gutmann donor number = 14.1, while for CH_2Cl_2 it is ranges from 0 to 1)[31,32] frequently leads to interactions with cationic species. This results in different oxidation potentials, or even differences in the number of electrons being transferred during redox processes. Such solvent effects are highlighted by the electrochemical oxidation of, for example, $Rh^I(\beta$-diketonato)(CO)(PPh_3)] in a one-electron transfer process to a Rh(II) species in

CH$_2$Cl$_2$ / [(^{n}Bu$_4$)N][BF$_4$],[33] but in a two-electron transfer process to a Rh(III) species in CH$_3$CN / [(^{n}Bu$_4$)N][PF$_6$].[34] Potential referencing in different solvents and electrolytes has to be made with care. Results in this work are referenced to FcH/FcH$^+$ as required by IUPAC, but the internal standard was not free ferrocene to prevent peak overlaps with **1 – 4**. Hence decamethylferrocene, Fc* was used as internal standard and potentials was thereafter adjusted to be versus FcH/FcH$^+$. Under our conditions the formal reduction potential of Fc* vs. FcH/FcH$^+$ is -550 mV in CH$_2$Cl$_2$ / [(^{n}Bu$_4$)N][PF$_6$], -610 mV in CH$_2$Cl$_2$ / [(^{n}Bu$_4$)N][B(C$_6$F$_5$)$_4$] and -510 mV in CH$_3$CN / [(^{n}Bu$_4$)N][PF$_6$].[35] It was found that in CH$_3$CN, **4** tungsten(0) oxidation is also a three electron transfer process, See Table 1 and Figure S3, Supplementary Information.

Scheme 2 shows the observed redox processes of **2** in the presence of [(^{n}Bu$_4$)N][PF$_6$]. This electrochemical scheme would also fit **4** if wave 1 is split into an "a" and "b" component. The monocarbene complexes **1** and **3** would fit the scheme if waves I$_a$ and/or I$_b$ are removed as required, and if wave 1 for **2** is rewritten to accommodate only one three electron transfer process rather than two. In the presence of [(^{n}Bu$_4$)N][B(C$_6$F$_5$)$_4$], the scheme would fit if the three-electron W$^{0/III}$ coupled is replaced with a two-electron W$^{0/II}$ couple.
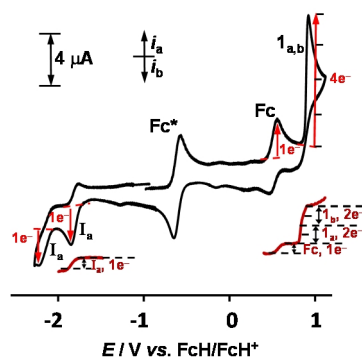
Figure 6. CV and LSV (brown curves) at 20 ^{o}C of 0.5 mmol·dm^{-3} solutions of **2** in CH$_2$Cl$_2$ / 0.2 mol·dm^{-3} [N(^{n}Bu)$_4$][B(C$_6$F$_5$)$_4$]. The number of electrons involved in each redox process is indicated next to the relevant waves. Each W is oxidized in a two-electron transfer process in this medium. Fc* = decamethylferrocene.

Further chemical reactions

↑

$[(OC)_5\overset{-}{W}{}^0-\overset{\bullet}{C}(OEt)\text{-}Fc'\text{-}(OEt)\overset{\bullet}{C}-\overset{-}{W}{}^0(CO)_5]$

+1e⁻
wave I_b ↑

$[(OC)_5\overset{-}{W}{}^0-\overset{\bullet}{C}(OEt)\text{-}Fc'\text{-}(OEt)C=W^0(CO)_5]$

+1e⁻ ⇵ **-1e⁻**
wave I_a

$[(OC)_5W^0=C(OEt)\text{-}Fc'\text{-}(OEt)C=W^0(CO)_5]$

+1e⁻ ⇵ **-1e⁻**
wave Fc

$[(OC)_5W^0=C(OEt)\text{-}\overset{+}{Fc'}\text{-}(OEt)C=W^0(CO)_5]$

-2 (3e⁻)
wave 1 ↓

$[(OC)_5\overset{3+}{W}{}^{III}=C(OEt)\text{-}\overset{+}{Fc'}\text{-}(OEt)C=\overset{3+}{W}{}^{III}(CO)_5]$

↓

Further chemical reactions
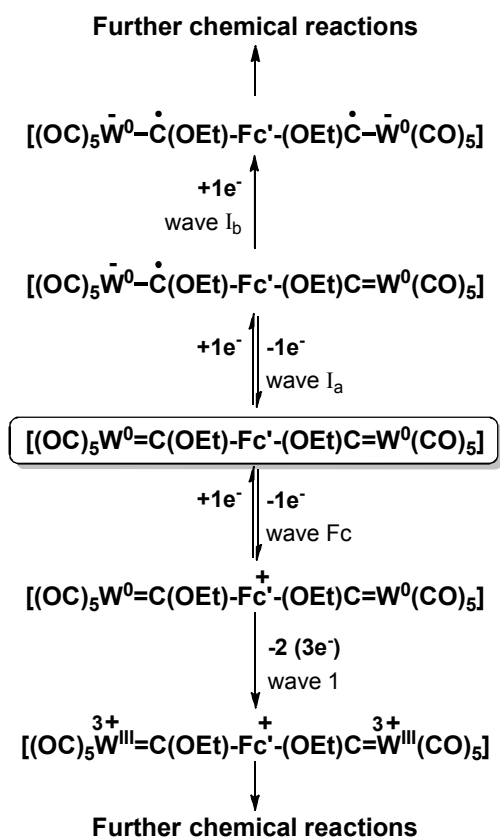
Scheme 2. Electrochemical reactions associated with **2**. Both the final reduction product possessing ⁻W-C• radical anions and the final oxidation product possessing two W(III) centers are highly reactive and undergo further chemical decomposition reactions.

The above described redox processes were finally addressed by means of a computational-DFT study. As shown in Figure 7, complex **1** is electrochemically oxidized to radical cation **1·⁺.** The computed spin density of this species indicates that the unpaired electron is located at the iron atom (1.26e), thus confirming that the first one-electron oxidation does not involve the tungsten center but the Fe(II) to Fe(III) reaction.
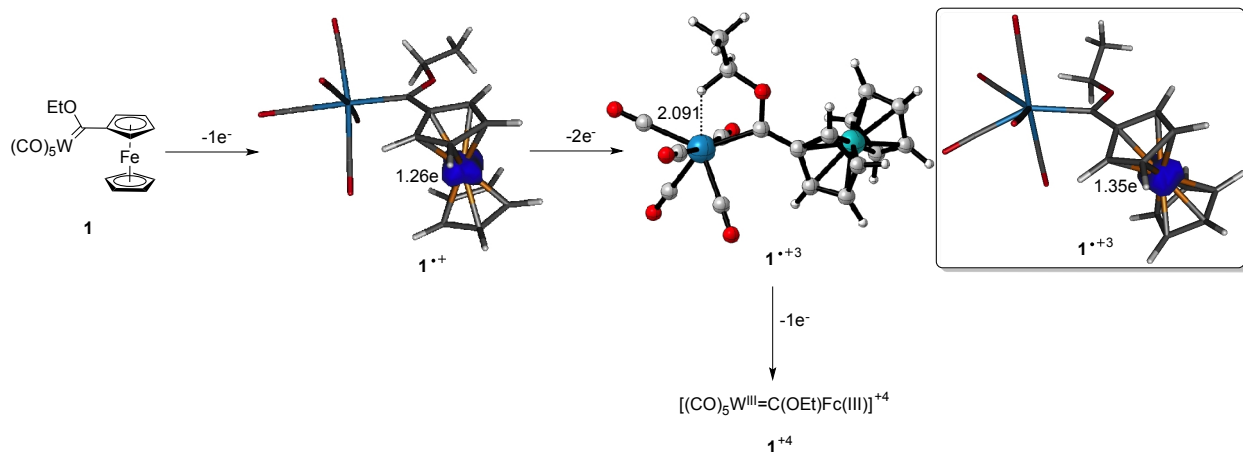
Figure 7. Computed oxidation process of complex **1** at the B3LYP/def2-SVP level. W···H bond distance in **1**·+3 is given in angstroms.

Subsequent 2-electron oxidation leads to the trication **1**·+3 whose unpaired electron remains at the iron atom (computed electron density on Fe of 1.35e). This indicates that the oxidation process involves the W(0) to W(II) reaction. As described above, the total three-electron tungsten oxidation process ends up with the third and final one-electron oxidation at the tungsten center (W(II) to W(III)) to form the corresponding tetracation **1**+4. Unfortunately, the structure of this open-shell singlet species (whose unpaired electrons are located at the iron and tungsten centers) could not be located on the potential energy surface (even using different functionals) due to convergence problems.

The structure of the trication **1**·+3 deserves further analysis. As shown in Figure 7, a hydrogen atom of the ethoxy substituent is found in close proximity to the tungsten atom (W···H distance of 2.091 Å), pointing to possible C−H···W agostic interaction. Indeed, the Laplacian distribution of **1**·+3 in the W···H−C plane (Figure 8) clearly reveals the occurrence of a bond critical point located between the transition metal and the hydrogen atom, which is associated with a bond

path running between the corresponding two atoms. This proves the existence of a direct interaction between both atoms. Moreover, the computed value of 0.045 e·Å^{-3} for the electron density at the bond critical point, is in the range expected for CH agostic interactions.[36] The structure of this species resembles that found for oxidised products of related chromium(0) carbene complexes upon 2-electron oxidation of the transition metal.[11] This peculiar bonding situation seems to be general for oxidized products of Fischer carbene complexes regardless of the transition metal involved and it implies the normal carbene structure is not retained after oxidation.
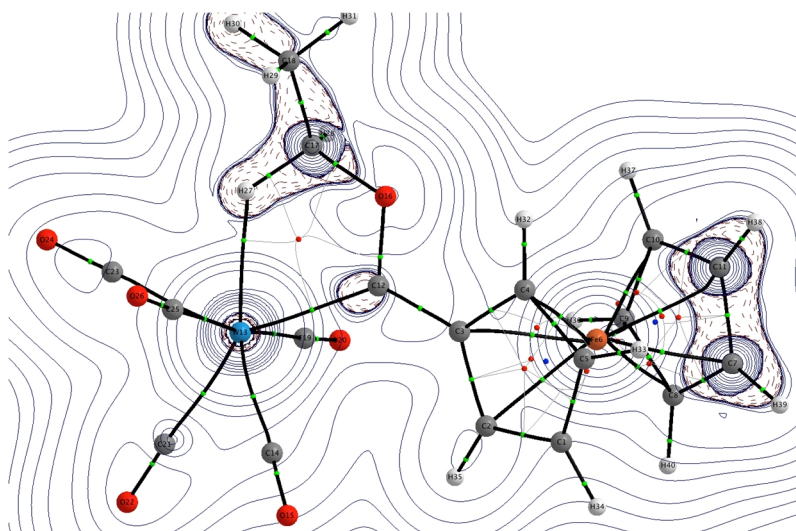
Figure 8. Contour line diagrams $\nabla^2\rho(r)$ for complex **1**$^{·+3}$ in the W−H−C plane. Solid lines indicate areas of charge concentration ($\nabla^2\rho(r) < 0$) while dashed lines show areas of charge depletion ($\nabla^2\rho(r) > 0$). The solid lines connecting the atomic nuclei are the bond paths while the small red spheres indicate the corresponding bond critical points. The solid lines separating the atomic basins indicate the zero-flux surfaces crossing the molecular plane.

Conclusion

Mono- and bis-ethoxycarbene and –butyl(or propyl)aminocarbene tungsten(0) complexes [$(CO)_5W=C(XR)Fc$], **1** and **3**, and [$(CO)_5W=C(XR)$-Fc'-$(XR)C=W(CO)_5$], **2** and **4** were prepared. For the aminocarbenes **3** and **4**, only the *syn*-rotamer possessing restricted rotation about the $C_{carbene}$-N bond was observed by ^{1}H NMR due to the steric bulk of the ferrocenyl carbene substituent. The chemically oxidized but short-lived ferrocenium complex [**1**$^+$]•**PF$_6$** was also synthesized. From an electrochemical study in CH_2Cl_2 / [($^nBu_4$)N][PF$_6$] it was found that the electron-rich carbene double bond functionality of all complexes were reduced from W=C to $^-$W-C• at potentials < -2.0 V vs FcH/FcH$^+$. This assignment was confirmed by DFT calculations, which indicate that the unpaired electron of the formed radical anion is mainly located on the carbene carbon atom. For the two biscarbene complexes **2** and **4**, reduction potentials of the two W=C functionalities were resolved which is indicative of good interactions between the formally carbene double bonds. The ferrocenyl group was electrochemically reversibly oxidized before W oxidation at potentials $0.206 < E^{o'} < 0.540$ V vs FcH/FcH$^+$. These potentials were continuously more than 250 mV smaller than those measured for the analogues Cr compounds. Tungsten(0) was oxidized in three consecutive but unresolved one-electron transfer steps to a W(III) species in the presence of [N(^nBu)$_4$][PF$_6$] as supporting electrolyte, or in CH_3CN as solvent. In CH_2Cl_2 containing [($^nBu_4$)N][B(C_6F_5)$_4$] as supporting electrolyte, tungsten(0) oxidation was found to be a two-electron transfer process. The structure of this tricationic W(II) species has been highlighted with DFT calculations. Complex **4** showed identifiable resolution between the oxidation of each W center. This also argued for a weak interaction between the two W centers. All redox assignments were mutually consistent with the computational data obtained at the DFT level, which suggest a peculiar bonding situation (i.e. stabilized by C−H⋯W agostic interaction)

in the tricationic species formed upon the oxidation process which involves the W(0) to W(II) reaction.

Experimental Section

General Procedures.

All manipulations involving organometallic compounds made use of standard Schlenk techniques under inert atmosphere. Solvents were dried over sodium metal (hexane, thf and diethylether) and phosphorouspentoxide (CH_2Cl_2); and distilled under nitrogen gas prior to use. All chemicals were used as purchased without further purification unless stated otherwise. Triethyloxoniumtetrafluoroborate was prepared according to literature procedures.[17] Purification of complexes was done with column chromatography using silica gel 60 (0.0063-0.200 mm) as the stationary phase. NMR spectra were recorded on a Bruker AVANCE 500 spectrometer. ^{1}H NMR spectra were recorded at 500.139 MHz and ^{13}C NMR at 125.75 MHz. The signals of the deuterated solvent were used as a reference: [1]H $CDCl_3$ at 7.24 ppm and C_6D_6 at 7.15 ppm; [13]C $CDCl_3$ at 77.00 ppm and C_6D_6 128.00 ppm. IR spectra were recorded on a Perkin-Elmer Spectrum RXI FT-IR spectrophotometer in solvent (hexane or DCM) as indicated. Only the vibration bands in the carbonyl-stretching region (ca. 1600-2200 cm^{-1}) were recorded.

[(CO)$_5$W=C(OEt)Fc] (1) was prepared according to previously reported methods.[15]

[(CO)$_5$W=C(OEt)Fc′(OEt)C=W(CO)$_5$] (2)

Dilithioferrocene was prepared according to literature procedures:[16] to a solution of ferrocene (4 mmol, 0.74g) in hexane was added TMEDA (8.2 mmol, 1.23 mL) and *n*BuLi in hexane (8.2 mmol) and stirred while heating to 60°C. After formation of the orange precipitate, the solvent

was removed *via* cannula filtration, and the precipitate redissolved in thf. $W(CO)_6$ (8 mmol, 2.81g) was added at -78°C, and stirred for 1 hour while allowing the reaction mixture to reach room temperature. The solvent thf was removed by reduced pressure and Et_3OBF_4 (8.2 mmol), dissolved in CH_2Cl_2, added at -30°C. After reaction completion, the solvent was evaporated. Column chromatography was used for purification and the dark red fraction collected. Yield: 2.65g (70%), black red crystals. Anal. Calcd for $W_2FeC_{26}H_{18}O_{12}$: C, 33.01; H, 1.92. Found: C, 31.98; H, 1.88. ^{1}H NMR ($CDCl_3$): δ 5.02 (m, 4H, $H_α$), 4.89 (q, J = 7.0 Hz, 4H, CH_2CH_3), 4.81 (m, 4H, $H_ß$), 1.61 (t, J = 7.1 Hz, 6H, CH_2CH_3). ^{13}C NMR ($CDCl_3$): δ n.o. ($C_{carbene}$), 201.91 (*trans*-CO), 197.58 (*cis*-CO) , 98.82 (C_{ipso}) , 74.52 ($C_α$), 69.15 ($C_β$) , 77.20 OCH_2), 14.12 (CH_3). IR (v_{CO}, cm^{-1}, CH_2Cl_2): 2060 m (A″$_1$), 1978 w (B), 1935 vs (A′$_1$ overlap E).

[(CO)₅W=C(NHBu)Fc] (3)

A diethylether solution of **1** (2 mmol, 1.13 g) was stirred at room temperature (rt) and *n*-butylamine (2 mmol, 0.20 mL) was added. The color changed rapidly from dark red to deep yellow. Purification was performed using column chromatography and a 1:1 mixture of hexane/CH_2Cl_2 as eluent. Yield: 0.90g (76%), yellow solid. Anal. Calcd for $WFeC_{20}H_{19}NO_5$: C, 40.50; H, 3.24. Found: C, 40.23; H, 3.09. ^{1}H NMR (C_6D_6): δ 8.91 (s, 1H, N**H**), 4.24 (br, 2H, $H_α$), 4.02 (br, 2H, $H_ß$), 3.86 (s, 5H, Cp), 3.53 (m, 2H, NCH_2), 1.35 (m, 2H, CH_2CH_2), 1.17 (m, 2H, CH_2CH_2), 0.78 (m, 3H, **CH₃**). ^{13}C NMR (C_6D_6): δ 249.14 ($C_{carbene}$), 203.27 (*trans*-CO), 199.27 (*cis*-CO) , 97.12 (C_{ipso}) , 71.12 ($C_α$), 69.86 ($C_β$ overlap Cp), 54.95 (NCH_2), 31.54 (CH_2CH_2), 20.07 (CH_2CH_2), 13.72 (**CH₃**). IR (v_{CO}, cm^{-1}, CH_2Cl_2): 2060 m (A″$_1$), 1966 w (B), 1922 vs (A′$_1$ overlap E).

[(CO)₅W=C(NHPr)Fc′(NHPr)C=W(CO)₅] (4)

Complex **2** (2 mmol, 1.89g) was dissolved in diethylether and *n*-propylamine (2 mmol, 0.16 mL) was added at rt. The color of the solution turned from dark red to deep yellow and volatiles were removed by reduced pressure. Purification was performed by employing column chromatography with a 1:1 hexane/CH_2Cl_2 solvent mixture.

Yield: 1.46g (75%), deep yellow crystals. Anal. Calcd for $W_2FeC_{28}H_{24}N_2O_{10}$: C, 34.59; H, 2.49. Found: C, 33.42; H, 2.35. ^{1}H NMR ($CDCl_3$): 8.96 (s, 2H, **H**N), 4.56 (m, 4H, H$_\alpha$), 4.48 (m, 4H, H$_\beta$), 3.88 (m, 4H, NC**H**$_2$), 1.86 (h, J = 7.4 Hz, 4H, C**H**$_2$CH$_3$), 1.13 (t, J = 7.4 Hz, 6H, C**H**$_3$). ^{13}C NMR (CDCl3): 249.58(C$_{carbene}$), 202.81 (CO$_{trans}$), 198.45 (CO$_{cis}$), 99.19 (C$_{ipso}$), 72.23 (C$_\alpha$), 70.15(C$_\beta$), 56.96 (HN**C**H$_2$), 23.01 (**C**H$_2$CH$_3$), 11.23 (**C**H$_3$). IR (ν_{CO}, cm^{-1}, CH_2Cl_2): 2060 m (A″$_1$), 1963 w (B), 1920 vs (A′$_1$ overlap E).

[(CO)$_5$W=C(OEt)Fc][PF$_6$] ([1$^+$]•PF$_6$)

Complex **1** (0.02g, 0.035 mmol) was dissolved in dichloromethane and cooled to -35°C. Silver hexafluorophosphate (0.009g, 0.035 mmol) was added and the solution changed from red to deep brown. The cold bath was removed and the brown solution was stirred at RT for 10 min. Cannula filtration was used to separate solids from the solution. ^{31}P NMR (CD_2Cl_2): δ -149.63 (h, J = 716.9, 706.7 Hz); ^{19}F NMR (CD_2Cl_2): δ -85.38 (d, J = 967.0 Hz); IR (ν_{CO}, cm^{-1}, CH_2Cl_2): 2074 (A$_1$″, m), 1996 (B, w), 1952 (A$_1$′ overlap E, vs).

Electrochemistry

Cyclic voltammograms (CV's), square wave voltammograms (SW's) and linear sweep voltammograms (LSV's) were recorded on a Princeton Applied Research PARSTAT 2273 voltammograph running PowerSuite (Version 2.58) utilizing a standard three-electrode cell in a M Braun Lab Master SP glovebox filled with high purity argon (H_2O and O_2 < 5 ppm) as

described before.[10,11] To establish whether the electrolyte used, $[(^nBu_4)N][PF_6]$, and also the solvent influenced the number of electrons transferred at the tungsten center, **4** was also studied in the presence of 0.2 mol dm^{-3} $[(^nBu_4)N][B(C_6F_5)_4]$[37] as supporting electrolyte and in CH_3CN as solvent. All electrode potentials are reported versus the ferrocene/ferrocenium redox couple $(FcH/FcH^+, FcH = Fe(\eta^5\text{-}C_5H_5)_2, E^{o\prime} = 0.00$ V) as reference.[38] However, decamethylferrocene, Fc*, was used as internal standard to prevent signal overlap with the ferrocenyl of **1 – 4**. Decamethylferrocene has a formal reduction potential of -550 mV versus free ferrocene with ΔE = 72 mV and i_{pc}/i_{pa} = 1 under the prevailing conditions utilizing CH_2Cl_2 / $[(^nBu_4)N][PF_6]$ as solvent / supporting electrolyte.[35] In the presence of $[(^nBu_4)N][B(C_6F_5)_4]$ as electrolyte, the decamethylferrocene potential moves to -610 mV versus free ferrocene, while in CH_3CN / $[(^nBu_4)N][PF_6]$ it moves to -510 mV.[35]

Computational details

Geometry optimizations without symmetry constraints were carried out using the Gaussian09 suite of programs[39] at the B3LYP (uB3LYP for open-shell species)[40] using the double-ζ plus polarization def2-SVP[41] basis set for all atoms. This protocol is denoted B3LYP/def2-SVP. All species were characterized by frequency calculations, and have a positive defined Hessian matrix indicating that they are minima on the potential energy surface.

All Atoms in Molecules (AIM)[42] results described in this work correspond to calculations performed at the B3LYP/6-31G(d)&WTBS level on the optimized geometries obtained at the B3LYP/def2-SVP level. The WTBS (well-tempered basis sets)[43], used herein to describe Fe and W, have been recommended for AIM calculations involving transition metals.[44] The topology of the ED was conducted using the AIMAll program package.[45]

AUTHOR INFORMATION

Corresponding Authors

Tel.: +27-12-420-2626; Fax: +27-(0)12-420-4687. *E-mail address:* daniela.bezuidenhout@up.ac.za (D.I. Bezuidenhout)

Tel.: +34-91-394-5155; Fax: +34-91-394-4310. *E-mail address*: israel@quim.ucm.es (I. Fernández)

Tel: +27-(0)51-401-2781; Fax: +27-(0)51-444-6384. *E-mail address*: swartsjc@ufs.ac.za (J.C. Swarts)

Author Contributions

The manuscript was written through contributions of all authors. All authors have given approval to the final version of the manuscript.

REFERENCES

(1) Pike A. R.; Ryder, L. C.; Horrocks, B. R.; Clegg, W.; Connolly, B. A.; Houlton, A. *Chem. Eur. J.* **2004**, *11*, 344-353.

(2) Spanig, F.; Kolvacs, C.; Hauke, F.; Ohlubo, K.; Fukuzumi, F.; Guldi, D. M.; Hirsch, A. *J. Am. Chem. Soc.* **2009**, *131*, 8180-8195.

(3) (a) Saravanakumar, D.; Sengottuvelan, N.; Narayanan, V.; Kandaswamy, M.; Varghese, T. L. *J. Appl. Polym. Sci.* **2011**, *119*, 2517-2524; (b) Jungbluth, H.; Lohmann, G. *Nachr. Chem. Tech. Lab*. **1999**, *47*, 534-538; (c) Swarts, P. J.; Immelman, M.; Lamprecht, G. J.; Greyling, S. E.; Swarts, J. C. *S. Afr. J. Chem.* **1997**, *50*, 208-216; (d) Shen, Q. L.; Shekhar, S.; Stambuli, J. P.; Hartwig, J. F. *Angew. Chem. Int. Ed.* **2005**, *44*, 1371-1375; (e) Conradie, J.; Swarts, J. C. *Organometallics*, **2009**, *28*, 1018-1026.

(4) (a) Shago, R. F.; Swarts, J. C.; Kreft, E.; Van Rensburg, C. E. J. *Anticancer Res*. **2007**, *27*, 3431-3434; (b) Van Rensburg, C. E. J.; Kreft, E.; Swarts, J. C.; Dalrymple, S. R.; Macdonald, D. M.; Cooke, M. W.; Aquino, M. A. S. *Anticancer Res*. **2002**, *22*, 889-892. (c) Gross, A.; Hüsken, N.; Schur, J.; Raszeja, L.; Ott, I.; Metzler-Nolte, N. *Bioconjugate Chemistry*, **2012**, *23*, 1764-1774. (d) Swarts, J. C.; Vosloo, T. G.; Cronje, S. J.; Du Plessis, W. C.; Van Rensburg, C. E. J.; Kreft, E.; Van Lier, J. E. *Anticancer Res.* **2008**, *28*, 2781-2784; (e) Ott, I.; Kowalski, K.; Gust, R.; Maurer, J.; Mücke, P.; Winter, R. F. *Bioorg. Med. Chem. Lett.* **2010**, *20*, 866-869.

(5) Recent reviews on the chemistry and applications of Fischer carbenes include: (a) Wu, Y.-T.; Kurahashi, T.; De Meijere, A. *J. Organomet. Chem.* **2005**, *690*, 5900-5911; (b) Gómez-Gallego, M.; Mancheño, M. J.; Sierra, M. A. *Acc. Chem. Res.* **2005**, *38*, 44-53; (c) Sierra, M. A.; Gómez-Gallego, M.; Martínez-Ávarez, R. *Chem.–Eur. J.* **2007**, *13*, 736-744; (d) Sierra, M. A.; Fernández, I.; Cossío, F. P. *Chem. Commun*. **2008**, 4671-4682; (e) Dötz, K. H.; Stendel, J. *Chem. Rev*. **2009**, *109*, 3227-3274; (f) Herndon, J. W. *Coord. Chem. Rev*. **2010**, *254*, 103-194; (g) Fernández-Rodríguez, M. A.; García-García, P.; Aguilar, E. *Chem. Comm*. **2010**, *46*, 7670-7687; (h) Fernández, I.; Cossío, F. P.; Sierra, M. A. *Acc. Chem. Res.* **2011**, *44*, 479-490; (i) Bezuidenhout, D. I.; Lotz, S.; Liles, D. C.; Van der Westhuizen, B. *Coord. Chem. Rev*. **2012**, *256*, 479-524; (j) Fernández, I.; Sierra, M. A. *Top. Heterocycl. Chem*. **2013**, *30*, 65-84.

(6) Representative examples: (a) Cases, M.; Frenking, G.; Duran, M.; Solà, M. *Organometallics,* **2002**, *21,* 4182-4191; (b) Poater, J.; Cases, M.; Fradera, X.; Duran, M.; Solà, M. *Chem. Phys.* **2003**, *294,* 129-139; (c) Fernández, I.; Cossío, F. P.; Arrieta, A.; Lecea, B.; Mancheño, M. J.; Sierra, M. A. *Organometallics* **2004**, *23,* 1065-1071; (d) Frenking, G.; Solà, M.; Vyboishchikov, S. F. *J. Organomet. Chem.* **2005**, *690,* 6178-6204; (e) Fernández, I.; Sierra, M. A.; Mancheño, M. J.; Gómez-Gallego, M.; Cossío, F. P. *Chem. Eur. J.* **2005**, *11,* 5988-5996; (f) Fernández, I.; Sierra, M. A.; Cossío, F. P. *J. Org. Chem.* **2008**, *73,* 2083-2089; (g) Valyaev, D. A.; Brousses, R.; Lugan, N.; Fernández, I.; Sierra, M. A. *Chem. Eur. J.* **2011**, *17,* 6602-6605; (h) Andrada, D. M.; Granados, A. M.; Solá, M.; Fernández, I. *Organometallics,* **2011**, *30,* 466-476.

(7) Connor, J. A.; Jones, E. M.; Lloyd, J. P. *J. Organomet. Chem.* **1970**, *24,* C20-C22.

(8) (a) Dötz, K. H.; Dietz, R.; Neugebauer, D. *Chem. Ber.* **1979**, *112,* 1486-1490; (b) Bennewits, J.; Nieger, M.; Lewall, B.; Dötz, K. H. *J. Organomet. Chem.* **2005**, *690,* 5892-5899.

(9) (a) Dötz, K. H. *Angew. Chem. Int. Ed. Engl.* **1975**, *14,* 644-645; (b) Wulff, W. D. in *Comprehensive Organic Synthesis,* Vol. 5 (Eds.: B. M. Trost, I. Fleming), Pergamon, Oxford, **1991**, p. 1065; (c) Minatti, A.; Dötz, K. H. *Top. Organomet. Chem.* **2004**, *13,* 123; (d) Waters, M. L.; Wulff, W. D. *Org. React.* **2008**, *70,* 121.

(10) Van der Westhuizen, B.; Swarts, P. J.; Strydom, I.; Liles, D. C.; Fernández, I.; Swarts, J. C.; Bezuidenhout, D. I. *Dalton Trans.* **2013**, *42,* 5367-5378.

(11) Van der Westhuizen, B.; Swarts, P. J.; Van Jaarsveld, L. M.; Liles, D. C.; Siegert, U.; Swarts, J. C.; Fernández, I.; Bezuidenhout, D. I. *Inorg. Chem.* **2013**, *52,* 6674-6684.

(12) (a) Bezuidenhout, D. I.; Van der Watt, E.; Liles, D. C.; Landman, M.; Lotz, S. *Organometallics,* **2008**, *27,* 2447-2456; (b) Bezuidenhout, D. I.; Lotz, S.; Landman, M.; Liles, D. C. *Inorg. Chem.* **2011**, *50,* 1521-1533.

(13) Baldoli, C.; Cerea, P.; Falciola, L.; Giannini, C.; Licandro, E.; Maiorana, S.; Mussini, P.; Perdicchia, D. *J. Organomet. Chem.* **2005**, *690*, 5777-5787.

(14) (a) Chu, G. M.; Fernández, I.; Sierra, M. A. *Chem. Eur. J.* **2013**, *19*, 5899-5908; (b) Hoskovcova, I.; Zverinova, R.; Radka, J.; Dvorak, D.; Tobrman, T.; Zalis, S.; Ludvik, J. *Electrochim. Acta,* **2011**, *56*, 6853-6859; (c) López-Alberca, M. P.; Mancheño, M. J.; Fernández, I.; Gómez-Gallego, M.; Sierra, M. A.; Hemmert, C.; Gornitzka, H. *Eur. J. Inorg. Chem.* **2011**, 842-849; (d) Bezuidenhout, D. I.; Barnard, W.; Van der Westhuizen, B.; Van der Watt, E.; Liles, D. C. *Dalton Trans.* **2011***, 40*, 1-11; (e) Hoskovcova, I.; Rohacova, J.; Dvorak, D.; Tobrman, T.; Zalis, S.; Zverinova, R.; Ludvik. R. *Electrochim. Acta* **2010**, *55*, 8341-8351; (f) Schobert, R.; Kempe, R,; Schmalz, T.; Gmeiner, A. *J. Organomet. Chem.* **2006**, *691*, 859-868; (g) Pombeiro, A. J. L. *J. Organomet. Chem.* **2005**, *690,* 6021-6040; (h) Fernández, I.; Mancheño, M. J.; Gómez-Gallego, M.; Sierra, M. A. *Org. Lett*. **2003**, *5*, 1237-1240; (i) Jayaprakash, K. N.; Ray, P. C.; Matsuoka, I.; Bhadbhade, M. M.; Puranik, V. G.; Das, P. K.; Nishihara, H.; Sarkar, A. *Organometallics* **1999**, *18*, 3851-3858; (j) Casey, C. P.; Albin, L. D.; Saeman, M. C.; Evans, D. H. *J. Organomet. Chem.* **1978**, *155*, C37-C40; (k) Lloyd, M. K.; McCleverty, J. A.; Orchard, D. G.; Connor, J. A.; Hall, M. B.; Hillier, I. H.; Jones, E. M.; McEwen, G. K. *J. Chem. Soc., Dalton* **1973**, 1743-1747.

(15) López-Cortés, J. G.; Contreras de la Cruz, L. F.; Ortega-Alfaro, M. C.; Toscano, R. A.; Alvarez-Toledano, C.; Rudler, H. *J. Organomet. Chem.* **2005**, *690*, 2229-2237.

(16) Sünkel, H.; Bernhartzeder, S. *J. Organomet. Chem.* **2011**, *696*, 1536-1540.

(17) Meerwein, H. *Org. Synth.* **1966**, *46*, 113–115.

(18) Inkpen, M. S.; Du, S.; Driver, M.; Albrecht, T.; Long, N. J. *Dalton Trans.* **2013**, *42*, 2813-2816.

(19) (a) Kvapilova, H.; Hoskovcova, I.; Kayanuma, M.; Daniels, C.; Zalis, S. *J. Phys. Chem. A* **2013**, *117*, 11456-11463; (b) Andrade, D. M.; Jimenez-Halla, J. O. C.; Sola, M. *J. Org. Chem.* **2010**, *75*, 5821-5836; (c) Garlichs-Zschoche, F. A.; Dotz, K. H. *Organometallics,* **2007**, *26*, 4535-4540; (d) Zheng, Z.; Yu, Z.; Luo, N.; Han, X. *J. Org. Chem.* **2006**, *71*, 9695-9700; (e) Bezuidenhout, D. I.; Liles, D. C.; Van Rooyen, P. H.; Lotz, S. *J. Organomet. Chem.*, **2007**, *692*, 774-783; (f) Klabunde, U.; Fischer, E. O. *J. Am. Chem. Soc.* **1967**, *89*, 7141-7142.

  (20) (a) Post, E. W.; Watters, K. L. *Inorg. Chim. Acta,* **1978**, *26*, 29-36; (b) Moser, E.; Fischer, E. O. *J. Organomet. Chem.*, **1968**, *15*, 147-155.

  (21) (a) Kemp, K. C.; Fourie, E.; Conradie, J.; Swarts, J. C. *Organometallics,* **2008**, *27*, 353-362; (b) Du Plessis, W. C.; Davis, W. L.; Cronje, S. J.; Swarts, J. C. *Inorg. Chim. Acta* **2001**, *314*, 97-104.

(22) Lage, M. L.; Fernández, I.; Mancheño, M. J.; Sierra, M. A. *Inorg. Chem.* **2008**, *47*, 5253-5258.

(23) Venkatasubbaiah, K.; Nowik, I.; Herber, R. H.; Jäkle, F. *Chem. Commun.* **2007**, 2154-2156.

(24) (a) Braterman, P. S. *Metal Carbonyl Spectra*; Academic Press Inc., London, **1975**, p 68. (b) Adams, D. M. *Metal-Ligand and Related Vibrations;* Edward Arnold Publishers Ltd., London, **1967**, p 98.

(25) (a) Gericke, H. J.; Barnard, N. I.; Erasmus, E.; Swarts, J. C.; Cook, M. J.; Aquino, M. A. S. *Inorg. Chim. Acta,* **2010**, *363*, 2222-2232; (b) Evans, D. H.; O'Connell, K. M.; Peterson, R. A.; Kelly, M. J. *J. Chem. Educ.*, **1983**, *60*, 290-293; *(c)* Kissinger, P. T.; Heineman, W. R. *J. Chem. Educ.* **1983**, *60*, 702-706. *(d)* Van Benschoten, J. J.; Lewis, J. Y.; Heineman, W. R. *J. Chem. Educ.*, **1983**, *60*, 772-776; *(e)* Mobbott, G. A. *J. Chem. Educ.*, **1983**, *60*, 697-702.

(26) Leading references are (a) Creutz, C.; Taube, H. *J. Am. Chem. Soc.* **1969**, *91*, 3988-3989. (b) Geiger, W. E.; Van Order, N.; Pierce, D. T.; Bitterwolf, T. E.; Reingold, A. L.; Chasteen, N. D. *Organometallics* **1991**, *10*, 2403-2411. (c) Van Order, N.; Geiger, W. E.; Bitterwolf, T. E.; Reingold, A. L. *J. Am. Chem. Soc.* **1987**, *109*, 5680-5690. (d) Pierce, D. T.; Geiger, W. E. *Inorg. Chem.* **1994**, *33*, 373-381. (e) Cook, M. J.; Chambrier, I.; White, G. F.; Fourie, E.; Swarts, J. C. *Dalton Trans.* **2009**, 1136-1144.

(27) For a review, see: Sierra, M. A.; Gómez-Gallego, M.; Martínez-Álvarez, R. *Chem-Eur. J.* **2007**, *13*, 736-744.

(28) Leading publications demonstrating the influence and use of $[(n\text{Bu}_4)\text{N}][\text{B}(\text{C}_6\text{F}_5)_4]$ and the complimentary role of associated *cations* with different charge densities may be found in (a) Barriere, F.; Kirss, R. U.; Geiger, W. E. *Organometallics* **2005**, *24*, 48-52 and references therein; (b) Hildebrandt, A.; Rüffer, T.; Erasmus, E.; Swarts, J. C.; Lang, H. *Organometallics* **2010**, *29*, 4900-4905; (c) Barriere, F.; Camire, N.; Geiger, W. E.; Mueller-Westerhoff, U. T.; Sanders, R. *J. Am. Chem. Soc.* **2002**, *124*, 7262-7263; (d) Barriere, F.; Geiger, W. E. *J. Am. Chem. Soc.* **2006**, *128*, 3980-3989; (e) Nafady, A.; Chin, T. T.; Geiger, W. E. *Organometallics* **2006** *25*, 1654-1663; (f) Chong, D. S.; Slote, J.; Geiger, W. E. *J. Electroanal. Chem.*, **2009**, *630*, 28-34.

(29) Swarts, J. C.; Nafady, A.; Roudebush, J. H.; Trupia, S.; Geiger, W. E. *Inorg. Chem.* **2009**, *48*, 2156-2165.

(30) Ruthenocene and osmocene behave quite similarly in that oxidation generates a Ru(IV) and Os(IV) species: (a) Watanabe, M.; Motoyama, I.; Takayama, T.; Sato, M. *J. Organomet. Chem.* **1997**, *549*, 13-23; (b) Watanabe, M.; Motoyama, I.; Shimoi, M.; Sano, H. *J. Organomet. Chem.* **1996**, *517*, 115-121; (c) Smith, T. P.; Iverson, D. J.; Droege, M. W.; Kwan, K. S.; Taube, H. *Inorg. Chem.* **1987**, *26*, 2882-2884.

(31) The donor number of CH_2Cl_2 is difficult to find in literature, it is always listed as an undetermined quantity. However, a Google search of the World Wide Web gave a value of 1, see http://www.stenutz.eu/chem/solv21.php. Leading references to Gutmann donor numbers include: (a) Gutmann, V. *Coord. Chem. Rev.*, **1976**, *18*, 225-255; (b) Gutmann, V. *The Donor-acceptor Approach to Molecular Interactions*, Plenum Press, New York, **1978**, p.20; (c) Huheey, J. E. *Inorganic Chemistry: Principles of structure and reactivity*, 3rd Ed., Harper, Cambridge, **1983**, p340.

(32) For a scale of donor numbers referenced to 1,2-dichloroethane, where CH_2Cl_2 has DN = 0 and MeCN has DN = 0.36, see: Reichardt, C. *Solvents and Solvent-Effects in Organic Chemistry,* 3rd Ed., Wiley-VCH, Weinheim, **2003**.

(33) Da Silva, M. F. C. G.; Trzeciak, A. M.; Ziolkowski, J. J.; Pombeiro, A. J. L. *J. Organomet. Chem.* **2001**, *620*, 174-181.

(34) (a) Conradie, J.; Swarts, J. C. *Eur. J. Inorg. Chem.* **2011**, 2439-2449; (b) Conradie, J.; Cameron, T. S.; Aquino, M. A. S.; Lamprecht, G. J.; Swarts, J. C. *Inorg. Chim. Acta* **2005**, 2530-2542.

(35) Leading references describing the electrochemical activity and behaviour of ferrocene and decamethylferrocene in a multitude of organic solvents are (a) Noviandri, I.; Brown, K. N.; Fleming, D. S.; Gulyas, P. T.; Lay, P. A.; Masters, A. F.; Phillips, L. *J. Phys. Chem. B* **1999**, *103*, 6713-6722; (b) Connelly, N. G.; Geiger, W. E. *Chem. Rev.* **1996**, *96*, 877-910; (c) Ruiz, J.; Astruc, D. *C.R. Acad. Sci.* (Paris), Ser. IIc 1, **1998**, 21-27; (d) Aranzaes, R. J.; Daniel, M. C.; Astruc, D. *Can. J. Chem.* **2006**, *84*, 288-299; (e) Fourie, E.; Swarts, J. C.; Chambrier, I.; Cook, M. J. *Dalton Trans.,* **2009**, 1145-1154.

(36) Lein, M. *Coord. Chem. Rev.* **2009**, *253*, 625-634.

(37) LeSuer, R. J.; Buttolph, C.; Geiger, W. E. *Anal. Chem.* **2004**, *76*, 6395-6401.

(38) (a) Gritzner, G.; Kuta, J. *Pure Appl. Chem.* **1984**, *56*, 461-466; (b) Gagne, R. R.; Koval, C. A.; Lisensky, G. C. *Inorg. Chem.* **1980**, *19*, 2854-2855.

(39) *Gaussian 09*, Revision B.1, Frisch, M. J.; Trucks, G. W.; Schlegel, H. B.; Scuseria, G. E.; Robb, M. A.; Cheeseman, J. R.; Scalmani, G.; Barone, V.; Mennucci, B.; Petersson, G. A.; Nakatsuji, H.; Caricato, M.; Li, X.; Hratchian, H. P.; Izmaylov, A. F.; Bloino, J.; Zheng, G.; Sonnenberg, J. L.; Hada, M.; Ehara, M.; Toyota, K.; Fukuda, R.; Hasegawa, J.; Ishida, M.; Nakajima, T.; Honda, Y.; Kitao, O.; Nakai, H.; Vreven, T.; Montgomery, Jr., J. A.; Peralta, J. E.; Ogliaro, F.; Bearpark, M.; Heyd, J. J.; Brothers, E.; Kudin, K. N.; Staroverov, V. N.; Kobayashi, R.; Normand, J.; Raghavachari, K.; Rendell, A.; Burant, J. C.; Iyengar, S. S.; Tomasi, J.; Cossi, M.; Rega, N.; Millam, N. J.; Klene, M.; Knox, J. E.; Cross, J. B.; Bakken, V.; Adamo, C.; Jaramillo, J.; Gomperts, R.; Stratmann, R. E.; Yazyev, O.; Austin, A. J.; Cammi, R.; Pomelli, C.; Ochterski, J. W.; Martin, R. L.; Morokuma, K.; Zakrzewski, V. G.; Voth, G. A.; Salvador, P.; Dannenberg, J. J.; Dapprich, S.; Daniels, A. D.; Farkas, Ö.; Foresman, J. B.; Ortiz, J. V.; Cioslowski, J.; Fox, D. J. Gaussian, Inc., Wallingford CT, **2009**.

(40) (a) Becke, A. D. *J. Chem. Phys.* **1993**, *98*, 5648-5652. (b) Lee, C.; Yang, W.; Parr, R. G. *Phys. Rev. B* **1988**, *37*, 785-789.

(41) Weigend, F.; Ahlrichs, R. *Phys. Chem. Chem. Phys.* **2005**, *7*, 3297-3305.

(42) Bader, R. F. W. *Atoms in Molecules. A Quantum Theory*; Oxford University Press: Oxford, U.K., **1990**.

(43) (a) Huzinaga, S.; Miguel, B. *Chem. Phys. Lett.* **1990**, *175*, 289-291. (b) Huzinaga, S.; Klobukowski, M. *Chem. Phys. Lett.* **1993**, *212*, 260-264.

(44) (a) Cabeza, J. A.; Van der Maelen, J. F.; García-Granda, S. *Organometallics* **2009**, *28*, 3666-3672. (b) Buil, M. L.; Esteruelas, M. A.; Fernández, I.; Izquierdo, S.; Oñate, E. *Organometallics* **2013**, *32*, 2744-2752.

(45) Keith, T. A. AIMAll, 2010, http://tkgristmill.com

ASSOCIATED CONTENT

Supporting Information.

The LSV and CV of complexes **1 - 4**, and Cartesian coordinates and energies of all the stationary species discussed in the text are included.
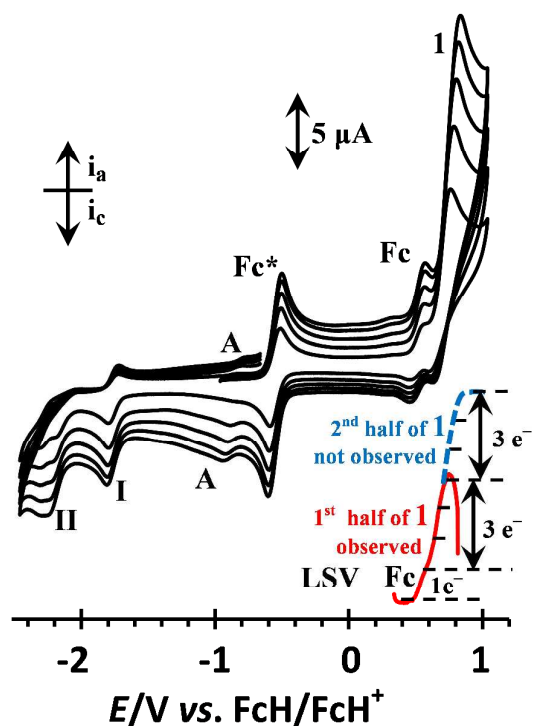
Figure S1. CV's of 0.5 mmol·dm^{-3} solutions of [(OC)$_5$W=C(OEt)-Fc'-(EtO)C=W(CO)$_5$], **2**, in CH$_2$Cl$_2$ containing 0.1 mol·dm^{-3} [N(^{n}Bu)$_4$][PF$_6$] as supporting electrolyte at a scan rate of 100 (smallest currents), 200, 300, 400 and 500 mV·s^{-1} and 20 ^{o}C. The LSV (1 mV·s^{-1}) show only the oxidation of the first W center in a three-electron transfer redox process, but compound stability is not enough to detect oxidation of the second W center on CV time scale. None of the three one-electron transfer steps of the oxidation of the first tungsten center can be resolved. The ferrocenyl group involves one-electron flow. From i$_{pc}$ values, the two resolved carbene reductions both involve a one electron reduction, but **2** is to unstable to detect carbene reduction on LSV time scale. Fc* = decamethylferrocene; peak A is a decomposition artefact because it was not present at the beginning of the CV measurement (scan rate 100 mV s^{-1}).
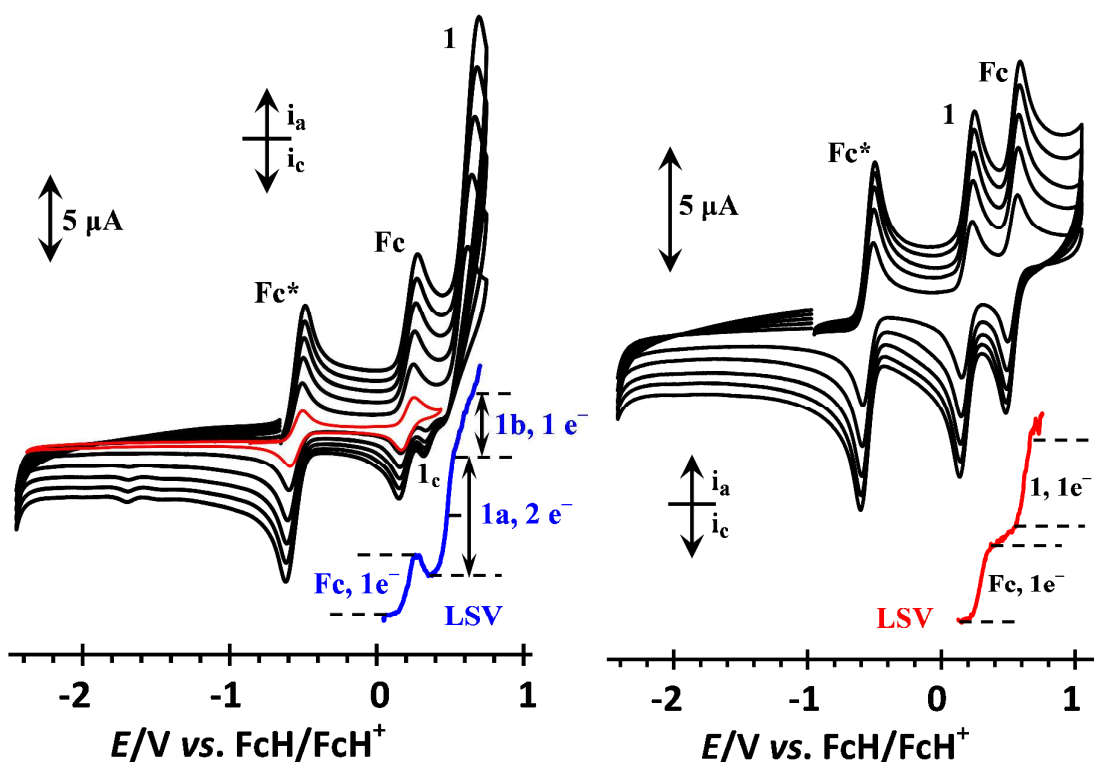
Figure S2. Left: CV's of 0.5 mmol dm^{-3} solutions of the **[(OC)$_5$W=C(Fc)(NHBu)]**, **3**, in CH$_2$Cl$_2$ containing 0.1 mol dm^{-3} [N(^{n}Bu)$_4$][PF$_6$] as supporting electrolyte at a scan rate of 100 (smallest currents), 200, 300, 400 and 500 mV s^{-1} and 20 ^{o}C. The LSV (1 mV s^{-1}) show the W center is ultimately involved in a three-electron transfer redox process, while the ferrocenyl group involves one-electron flow. The first two electrons during tungsten oxidation cannot be resolved, but the third follows slower after the first two on LSV timescale. In addition, the W(0) moiety at wave 1 is oxidised *after* the ferrocenyl group. Fc* = decamethylferrocene. Right: CV's and LSV's of **[(OC)$_5$Cr=C(Fc)(NHBu)]** under the same conditions. In contrast to the tungsten eqiuivalent, it is notable that Cr(0) involves a one-electron oxidation at wave 1 *before* oxidation of the ferrocenyl group. The electrochemically generated Cr(I) species do undergo a second one-electron oxidation to generate Cr(II) but this occurs at potentials outside the solvent window.

Figure S3. Voltammograms at 20 °C of 0.5 mmol dm^{-3} solutions of **4**, in (a) CH$_2$Cl$_2$ / 0.1 mol dm^{-3} [N(^{n}Bu)$_4$][PF$_6$] (green CV at 300 mV s^{-1}), (b) in CH$_2$Cl$_2$ / 0.2 mol dm^{-3} [N(^{n}Bu)$_4$][B(C$_6$F$_5$)$_4$] (black CV at 500 mV s^{-1}, black LSV at 1 mV s^{-1}, black SW at 20 Hz, orange SW' and brown SW"), and in (c) CH$_3$CN / 0.2 mol dm^{-3} [N(^{n}Bu)$_4$][PF$_6$] (red CV at 100 mV s^{-1} and red LSV at 1 mV s^{-1}). The number of electrons involved in W oxidation is indicated next to the relevant waves. In [N(^{n}Bu)$_4$][B(C$_6$F$_5$)$_4$] (black CV and LSV), W is oxidized in a 2-electron process. In the presence of CH$_3$CN (red CV and LSV) or [N(^{n}Bu)$_4$][PF$_6$], W is oxidized in a 3-electron process. Fc* = decamethylferrocene, SW' and SW" is the first and second derivative of the SW curve, differentiated over 4 mV intervals; currents were scaled to allow easy observation of peaks.

Discussion on Figure S3: Assignment of a 2-electron or 3-electron process for W oxidation in the case of **4** was difficult due to the closeness of the peaks labeled (Fc+1$_a$) and 1$_b$. A two-electron assignment fitted CV peak currents and LSV traces marginally better than a three-electron assignment but was by no means beyond all reasonable doubt. However, in analogy to **1**, **2**, and **3**,

we also assign a two-electron process to W(0) oxidation for **4**. In an attempt to see if it is not possible to separate electron transfer events more we also collected SW data for **4** because it is known that SW can sometimes separate closely-overlapping peaks, especially for reversible processes, better. We also obtained the first and second derivative of the SW curve to see if that would not allow better peak separation. It did not.

Figure 3S shows CV's of **4** overlaid under the following conditions:
(a) in CH_2Cl_2 / 0.1 mol dm^{-3} [N(^{n}Bu)$_4$][PF$_6$] (green CV at 300 mV s^{-1}),
(b) in CH_2Cl_2 / 0.2 mol dm^{-3} [N(^{n}Bu)$_4$][B(C$_6$F$_5$)$_4$] (black CV at 500 mV s^{-1}, black LSV at 1 mV s^{-1}, black SW at 20 Hz, orange SW' and brown SW''), and in
(c) CH$_3$CN / 0.2 mol dm^{-3} [N(^{n}Bu)$_4$][PF$_6$] (red CV at 100 mV s^{-1} and red LSV at 1 mV s^{-1}).

Also shown are the LSV's of conditions (b) and (c), and well enlarged, the SW, the first derivative of the SW (i.e $\left(\dfrac{\partial i}{\partial E}\right)_T = SW'$, orange) and the second derivative of the SW voltammogram (i.e. $\left(\dfrac{\partial^2 i}{\partial E^2}\right)_T = SW''$, brown). The first obvious difference between these three mediums is that in CH$_3$CN, or in CH_2Cl_2 but in the presence of [(^{n}Bu$_4$)N][B(C$_6$F$_5$)$_4$] as supporting electrolyte, resolution between the two W(0) oxidations are markedly increased. Differences in oxidation potentials between the "a" and "b" components of $W^{0/III}$ oxidation of **4** in CH_2Cl_2 or CH$_3$CN / [(^{n}Bu$_4$)N][PF$_6$] are $\Delta E^{o'} = E_{pa,W(0)\ oxd\ 1b} - E_{pa,W(0)\ oxd\ (Fc+1a)} = 51$ and 337 mV respectively. In CH_2Cl_2 / [(^{n}Bu$_4$)N][B(C$_6$F$_5$)$_4$], $\Delta E^{o'} = 212$ mV. Because $\Delta E^{o'} = 51$ mV is too far from zero to allow disregarding of the decay current, but at the same time it is too small to construct an accurate decay current to measure i_{pa} for wave 1b, CV peak currents could not clearly distinguish between a $W^{0/III}$ or a $W^{0/II}$ couple for **4**. The LSV shown in Figure 4S for the CH_2Cl_2 / [(^{n}Bu$_4$)N][B(C$_6$F$_5$)$_4$] medium favored a $W^{0/II}$ process. The SW favours a $W^{0/II}$ couple because the shoulders 1$_{b1}$ and 1$_{b2}$ are considered accurate and real (not an artifact) thus indicating two consecutive one-electron transfer processes.

The first derivative of the SW, the curve labeled as SW' in Figure 4S, only highlighted wave 1$_{b2}$ and one of the peaks in wave "Fc+1$_{a1-2}$" where it crossed the X-axis, but the second derivative curve labeled as SW'' also showed waves 1$_{b1}$ and 1$_{b2}$ at the extremities of the negative peak. For the wave labeled as wave "Fc+1$_{a1-2}$", following the dotted lines in Figure 4S, all three components of this redox process *may* have been identified in curve SW'', but the shoulders associated with the first and last peak is so insignificant that it disallows conclusions with any degree of certainty. We conclude that even the use of the 1st and 2nd derivative does not really help to resolve closely overlapping peaks. This conclusion is consistent with those of Taube whom described much earlier the problems associated with resolving closely overlapping redox events (D.E. Richardson, H. Taube, *Inorg. Chem.* 1981, *20*, 1278-1285).

Lastly, from the red LSV in Figure 4S, acetonitrile also leads to a three-electron $W^{0/III}$ couple.
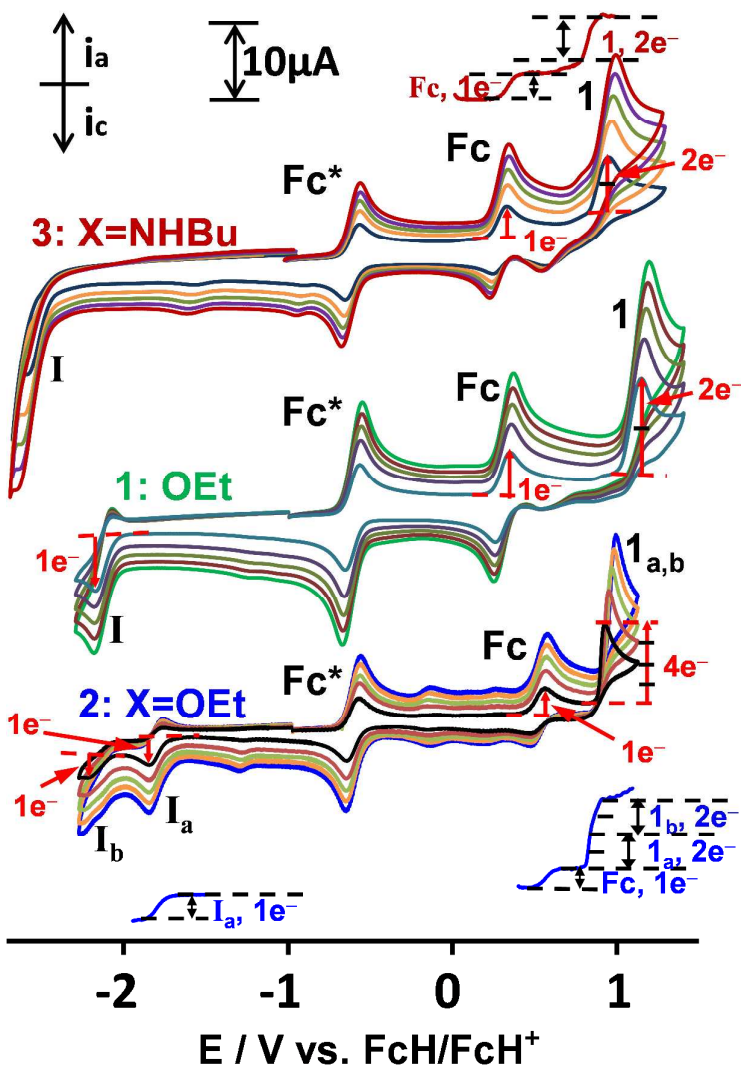
Figure S4. Cyclic voltammograms at 20 $^{\circ}$C of 0.5 mmol dm^{-3} solutions of [(CO)$_5$W=C(XR)Fc], **3** (XR = NHBu), **1** (XR = OEt), as well as [(CO)$_5$W=C(OEt)-Fc'-(OEt)C=W(CO)$_5$], **2** in CH$_2$Cl$_2$ / 0.2 mol dm^{-3} [N(^{n}Bu)$_4$][B(C$_6$F$_5$)$_4$]. The number of electrons involved in oxidation is indicated next to the relevant waves. It is clear that in this medium and supporting electrolyte, tungsten is oxidised in a two-electron process, NOT a three-electron process as was the case in CH$_2$Cl$_2$ / 0.2 mol dm^{-3} [N(^{n}Bu)$_4$][PF$_6$]. Fc* = decamethylferrocene.

Table S1. Cartesian coordinates (in Å) and total energies (in a. u., zero-point vibrational energy included) of all the stationary points discussed in the text. All calculations have been performed at the B3LYP/def2-SVP level.

1: E= -2474.567877

C	3.239641000	-1.333428000	-1.620702000
C	2.666014000	-0.064746000	-1.932106000
C	3.578149000	0.952653000	-1.512119000
C	4.719927000	0.309327000	-0.943430000
C	4.509957000	-1.102297000	-1.008469000
Fe	3.012241000	-0.203980000	0.112491000
C	1.622032000	-1.120445000	1.338988000
C	1.291500000	0.276114000	1.161592000
C	2.426047000	1.035430000	1.650780000
C	3.398322000	0.123531000	2.136831000
C	2.904526000	-1.203550000	1.941542000
C	0.092347000	0.860503000	0.554979000
O	0.279784000	2.176271000	0.484215000
C	-0.681690000	3.096324000	-0.045558000
C	-0.074728000	4.483936000	0.002233000
W	-1.721158000	-0.286413000	-0.040500000
C	-0.574523000	-1.754526000	-0.993646000
O	0.024110000	-2.589560000	-1.524500000
C	-3.386521000	-1.457773000	-0.524111000
O	-4.304501000	-2.108322000	-0.789297000
C	-1.979573000	0.684473000	-1.877416000
O	-2.158319000	1.199636000	-2.898075000
C	-3.087481000	1.049973000	0.822447000
O	-3.883013000	1.756251000	1.275429000
C	-1.614320000	-1.339215000	1.774666000
O	-1.570930000	-1.937161000	2.759706000
H	-1.598571000	3.040254000	0.559123000
H	-0.931692000	2.801480000	-1.075277000
H	0.174411000	4.770670000	1.035337000
H	-0.794284000	5.216248000	-0.394863000
H	0.841671000	4.536632000	-0.605353000
H	2.496193000	2.119573000	1.650932000
H	4.365233000	0.388587000	2.562355000
H	3.429463000	-2.125023000	2.188748000
H	1.005180000	-1.969828000	1.063412000
H	1.686397000	0.098939000	-2.378826000
H	3.425645000	2.027241000	-1.599699000
H	5.588929000	0.807396000	-0.515495000
H	5.191744000	-1.867988000	-0.640802000
H	2.772291000	-2.300761000	-1.796228000

3: E= -2533.234536

C	2.285623000	1.074706000	1.710135000
C	3.400137000	0.337049000	2.194599000
C	3.197965000	-1.036246000	1.864252000
C	1.957278000	-1.153011000	1.181937000
C	1.361035000	0.155217000	1.073533000
Fe	3.206536000	0.120017000	0.130746000
C	3.745802000	1.503931000	-1.319577000
C	4.909965000	0.877111000	-0.775248000
C	4.806733000	-0.527650000	-1.014978000
C	3.579742000	-0.771064000	-1.705504000
C	2.926037000	0.484006000	-1.894370000
C	0.075372000	0.518920000	0.430428000
W	-1.516764000	-1.002976000	-0.042783000
C	-2.067303000	-0.062797000	-1.827175000
O	-2.403110000	0.436940000	-2.816675000
N	-0.011701000	1.832591000	0.205747000
C	-1.122152000	2.601663000	-0.338447000
C	-1.172728000	4.005329000	0.265077000
C	-2.318980000	4.850915000	-0.298004000
C	-2.381890000	6.256846000	0.299483000
C	-3.023489000	0.037571000	0.978384000
O	-3.877019000	0.599167000	1.520814000
C	-1.077256000	-2.048796000	1.721549000
O	-0.853155000	-2.655309000	2.678592000
C	-0.157117000	-2.164339000	-1.127095000
O	0.581692000	-2.824140000	-1.726816000
C	-2.942064000	-2.465989000	-0.462788000
O	-3.732961000	-3.278406000	-0.696875000
H	-2.051778000	2.058533000	-0.130099000
H	-1.030522000	2.665075000	-1.437874000
H	-1.272488000	3.922270000	1.361941000
H	-0.212257000	4.523223000	0.077625000
H	2.147485000	2.145476000	1.856159000
H	4.257858000	0.752986000	2.721021000
H	3.882586000	-1.854953000	2.079533000
H	1.546613000	-2.078392000	0.791533000
H	1.956146000	0.629084000	-2.368557000
H	3.528599000	2.571257000	-1.302143000
H	5.726794000	1.380423000	-0.259766000
H	5.527624000	-1.283344000	-0.706299000
H	3.190780000	-1.740825000	-2.011959000
H	-2.215996000	4.918355000	-1.395945000
H	-3.274888000	4.328401000	-0.116308000
H	-3.216423000	6.835305000	-0.126359000
H	-2.524478000	6.222237000	1.392290000
H	-1.453480000	6.819365000	0.104196000
H	0.820519000	2.390917000	0.387898000

1˙⁻: E= -2474.628171

C	2.923592000	-0.930195000	2.058417000
C	1.648290000	-0.921970000	1.417974000

C	1.268589000	0.443765000	1.120399000
C	2.418970000	1.248569000	1.491154000
C	3.401389000	0.416633000	2.105328000
Fe	3.115775000	-0.171870000	0.153022000
C	4.599469000	-1.223661000	-0.896612000
C	3.314028000	-1.456502000	-1.481223000
C	2.788686000	-0.200461000	-1.914090000
C	3.736366000	0.812032000	-1.577363000
C	4.859451000	0.179742000	-0.951487000
C	0.056723000	0.929656000	0.516444000
W	-1.740987000	-0.316899000	-0.029992000
C	-1.641235000	-1.291756000	1.824865000
O	-1.626428000	-1.857118000	2.837893000
O	0.224470000	2.287527000	0.264072000
C	-0.874438000	3.141715000	0.065491000
C	-0.344256000	4.519562000	-0.297772000
C	-0.567110000	-1.818509000	-0.895026000
O	0.019519000	-2.687518000	-1.398040000
C	-3.354837000	-1.524197000	-0.504664000
O	-4.267230000	-2.206716000	-0.773220000
C	-1.941660000	0.573605000	-1.909541000
O	-2.088282000	1.043506000	-2.963853000
C	-3.159882000	1.009296000	0.738936000
O	-3.996402000	1.710100000	1.144513000
H	-1.489650000	3.197594000	0.984276000
H	-1.531897000	2.760921000	-0.734315000
H	0.300272000	4.915989000	0.503433000
H	-1.177447000	5.223837000	-0.455085000
H	0.252815000	4.473322000	-1.222535000
H	2.475929000	2.325543000	1.357350000
H	4.352728000	0.747732000	2.522696000
H	3.441822000	-1.812707000	2.433011000
H	1.041856000	-1.802253000	1.225181000
H	1.810414000	-0.039135000	-2.364427000
H	3.616507000	1.880531000	-1.751636000
H	5.749967000	0.682865000	-0.575362000
H	5.255261000	-1.981620000	-0.468850000
H	2.806319000	-2.415635000	-1.571173000

1·⁺: E= -2474.330179

C	2.884547000	-1.002186000	2.028406000
C	1.609294000	-0.991918000	1.392099000
C	1.224161000	0.372133000	1.145857000
C	2.315163000	1.190816000	1.604122000
C	3.323858000	0.353630000	2.155216000
Fe	3.095912000	-0.159537000	0.135500000
C	4.619051000	-1.177073000	-0.895934000
C	3.394274000	-1.387530000	-1.600100000
C	2.905141000	-0.120223000	-2.020158000
C	3.815378000	0.880767000	-1.576846000
C	4.882725000	0.230462000	-0.882106000

C	-0.009910000	0.906674000	0.510890000
W	-1.736257000	-0.309536000	-0.037279000
C	-1.578211000	-1.393961000	1.759411000
O	-1.492011000	-2.007294000	2.727974000
O	0.172757000	2.224736000	0.405494000
C	-0.826119000	3.124506000	-0.103355000
C	-0.264443000	4.529662000	-0.068533000
C	-0.504953000	-1.725936000	-0.951133000
O	0.178533000	-2.515155000	-1.448600000
C	-3.361163000	-1.584438000	-0.522490000
O	-4.234067000	-2.280456000	-0.783983000
C	-2.120325000	0.657723000	-1.868953000
O	-2.369448000	1.154319000	-2.876398000
C	-3.192212000	0.982997000	0.790194000
O	-4.022031000	1.650849000	1.218308000
H	-1.726107000	3.035690000	0.523451000
H	-1.087155000	2.817459000	-1.127494000
H	-0.008083000	4.829989000	0.958565000
H	-1.017678000	5.234302000	-0.451864000
H	0.634078000	4.616042000	-0.698296000
H	2.344900000	2.275227000	1.530843000
H	4.260710000	0.688538000	2.599621000
H	3.421353000	-1.889751000	2.361316000
H	1.033399000	-1.879005000	1.145638000
H	1.966174000	0.055926000	-2.544569000
H	3.711005000	1.954079000	-1.732345000
H	5.747666000	0.718217000	-0.433891000
H	5.244213000	-1.952222000	-0.453948000
H	2.897444000	-2.343441000	-1.763254000

1^{2+}: E= -2473.449333

C	2.938244000	-1.496601000	1.728851000
C	1.804275000	-1.354209000	0.895845000
C	1.391390000	0.036169000	0.926951000
C	2.366586000	0.740283000	1.755621000
C	3.269784000	-0.216299000	2.268927000
Fe	3.368996000	-0.115576000	0.080959000
C	5.341812000	-0.477889000	-0.510519000
C	4.450149000	-1.049597000	-1.474817000
C	3.692524000	0.013742000	-2.046574000
C	4.116075000	1.238540000	-1.446121000
C	5.132375000	0.940228000	-0.499260000
C	0.173582000	0.642049000	0.432988000
W	-1.856954000	-0.132963000	-0.103298000
C	-1.317524000	-1.795289000	1.120380000
O	-1.053398000	-2.652277000	1.814543000
O	0.252118000	1.954360000	0.349627000
C	-0.859637000	2.629152000	-0.249054000
C	-1.193707000	3.930273000	0.427998000
C	-0.985825000	-0.365220000	-2.035259000
O	-0.506124000	-0.474025000	-3.060856000

C	-2.962017000	-1.863627000	-0.810238000
O	-3.511259000	-2.764993000	-1.215423000
C	-3.773399000	0.657582000	-0.844494000
O	-4.752757000	1.081908000	-1.208173000
C	-2.782849000	0.348180000	1.773850000
O	-3.270987000	0.620022000	2.760337000
H	-1.813161000	1.957579000	-0.081313000
H	-0.679552000	2.722876000	-1.330604000
H	-1.417112000	3.801751000	1.496668000
H	-2.044060000	4.415888000	-0.075185000
H	-0.322820000	4.600916000	0.320153000
H	2.345194000	1.801041000	2.005212000
H	4.101664000	-0.006175000	2.944325000
H	3.484364000	-2.425155000	1.906145000
H	1.339110000	-2.164053000	0.334341000
H	2.927822000	-0.090606000	-2.817474000
H	3.723013000	2.232742000	-1.664185000
H	5.658198000	1.661703000	0.128855000
H	6.067670000	-1.022322000	0.096530000
H	4.378561000	-2.106758000	-1.735239000